Real Solid and Liquid Bodies 6

W. Demtröder, *Mechanics and Thermodynamics*, Undergraduate Lecture Notes in Physics, DOI 10.1007/978-3-319-27877-3_6

In this chapter, we will proceed with the stepwise refinement of our "*model of reality*". We will take into account the experimental fact that extended bodies can change their shape under the influence of external forces. We will also *discuss* the important question why and under which conditions real bodies can exist in different aggregation states as solids, liquids or gases. We will see, that an atomic model, which considers the different interactions between the atoms, can at least qualitatively explain all observed phenomena. For a quantitative description, a more profound knowledge about the atomic structure is demanded. The quantitative calculation of the detailed characteristics of solids or liquids is still not trivial, even with fast computers and sophisticated programs, because of the enormous number (10^{23} /kg) of atoms involved. Here symmetry considerations are helpful to facilitate the description.

If all physical characteristics of an extended body (density, elasticity, hardness etc.) are constant within the body, we call it a **homogeneous body**. Are they also independent of the direction the body is **isotropic**. A liquid metal is an example of an isotropic and homogeneous body while a NaCl-crystal (table salt) is homogeneous but not isotropic.

6.1 Atomic Model of the Different Aggregate States

Many experiments have proved that all macroscopic bodies are composed of atoms or molecules (see Vol. 3). Between two atoms, which consist of a positively charged small nucleus and a negatively charged extended electron cloud, attractive as well as repulsive interactions can occur. The superposition of all these interactions results in a force $\boldsymbol{F}(r)$ and a potential energy $E_\mathrm{p}(r)$ which depend on the distance r between the interacting atoms and which are qualitatively depicted in Fig. 6.1. At the equilibrium distance r_0, the potential energy $E_\mathrm{p}(r)$ shows a minimum and the force $F(r) = -\operatorname{grad} E_\mathrm{p}$ becomes zero. For shorter distances $r < r_0$ the repulsive forces dominate and for larger distances $r > r_0$ the attractive forces. For both cases, the potential energy increases. When an atom A is surrounded by many other atoms A_i at distances r_i the total force $\boldsymbol{F}$ acting on A is the vector sum of all individual forces $\boldsymbol{F}_i$:

$$\boldsymbol{F} = \sum \boldsymbol{F}_i(r_i) \; .$$

The resulting potential energy E_p of atom A depends on the spatial distribution of the surrounding atoms A_i and is related to the force F by $\boldsymbol{F} = -\mathbf{grad}\, E_\mathrm{p}$.

In *crystalline solids* the atoms are arranged in regular lattices (Fig. 6.2) while in *amorphous solids* they sit on more or less statistically distributed sites. Examples for the first cases are NaCl-crystals, or noble gas crystals at low temperatures, while examples for amorphous solids are glasses or amorphous silicon, which is used for solar cells.

When we place the atom A in a crystalline solid at the origin $\boldsymbol{r} = \mathbf{0}$ of our coordinate system the atoms A_i have the position

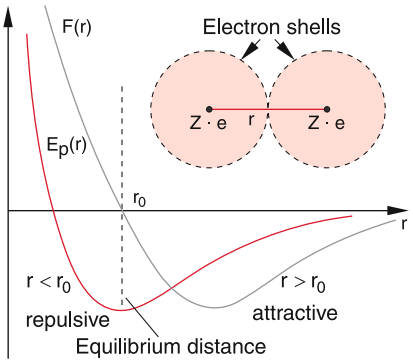

Figure 6.1 Qualitative dependence of potential energy $E_p(r)$ and force $F(r)$ between two atoms as a function of distance r between the nuclei of two adjacent atoms

vectors

$$\boldsymbol{r}_i = n_{1i}\,\boldsymbol{a} + n_{2i}\,\boldsymbol{b} + n_{3i}\,\boldsymbol{c} \; , \tag{6.1}$$

where the $n_{\alpha i}$ are integers and the basis vectors $\boldsymbol{a}, \boldsymbol{b}, \boldsymbol{c}$ define the unit cell (or elementary cell) in the crystalline solid. They are marked as red vectors in Fig. 6.2. Their magnitudes and directions define the crystal structure of the solid. The forces between the atoms can be modelled by elastic springs (Fig. 6.3) where the restoring force constants k_i can be different in the different directions. At the absolute temperature T the atoms vibrate about their equilibrium position r_0. Their mean kinetic energy is $\langle E_\mathrm{kin} \rangle = (1/2)kT$ per degree of freedom (see Sect. 7.3) where the equilibrium positions correspond to the minimum of the potential energy E_p in Fig. 6.1. For temperatures far below the melting temperature, $\langle E_\mathrm{kin} \rangle$ is small compared to the magnitude $|E_\mathrm{p}(r_0)|$ of the potential energy at the equilibrium position which means that the atoms cannot leave their equilibrium positions.

If the temperature rises above the melting temperature the mean kinetic energy $\langle E_\mathrm{kin} \rangle$ becomes larger than the binding energy $E_B = -E_\mathrm{p}(r_0)$. The atoms cannot be kept any

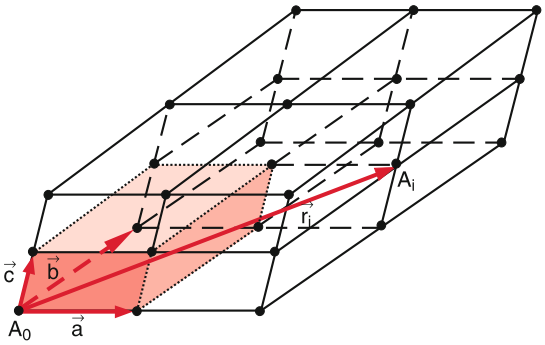

Figure 6.2 Regular structure of a solid crystal. The basis vectors $\boldsymbol{a}$, $\boldsymbol{b}$, $\boldsymbol{c}$ form the elementary cell with volume $V_E = (\boldsymbol{a} \times \boldsymbol{b}) \cdot \boldsymbol{c}$. The position vector of the point A is $\boldsymbol{r}_A = 2\boldsymbol{a} + \boldsymbol{b} + \boldsymbol{c}$

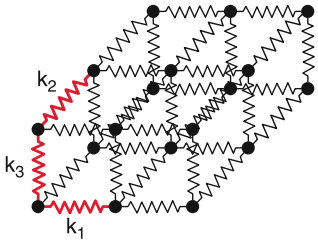

Figure 6.3 Spring model of a solid crystal. The restoring force is for an isotropic crystal equal for all three directions ***a***, ***b***, ***c***, for an unisotropic crystal they differ

longer on their positions r_i but can diffuse around. The crystalline solid melts and converts to the liquid state.

Also in the liquid state the minimum of the potential energy remains at the mean distance $\langle r_0 \rangle$ between the atoms. This means that the density in the liquid state is not very different from that in the solid state. However, now a single atom is no longer bound to a fixed position but can move freely within the liquid. Nevertheless, there is still a certain order. If one plots the probability $W(r)$ that an atom A occupies a position with the distance r from its neighbors (Fig. 6.4) a pronounced maximum is found at $r = r_0$ which is close to the minimum distance r_0 in the crystalline solid. Similar to the amorphous solid the liquid has a *short range order*, while a crystalline solid has a *long range order*, because it is possible to assign a definite position $r = n_1 a + n_2 b + n_3 c$ (with integers n_i) to each atom regardless how far away it is (Fig. 6.2). While the crystalline solid can be described by the spring model of Fig. 6.3, many features of liquids can be modelled by the string model of Fig. 6.5. Here the atoms are connected by strings of constant lengths where the directions can be arbitrarily altered. The balls in this mechanical model can move similar to the atoms in a liquid.

A further increase of the temperature above the boiling point makes the mean kinetic energy large compared to the magnitude of the potential energy. The potential energy is then negligible

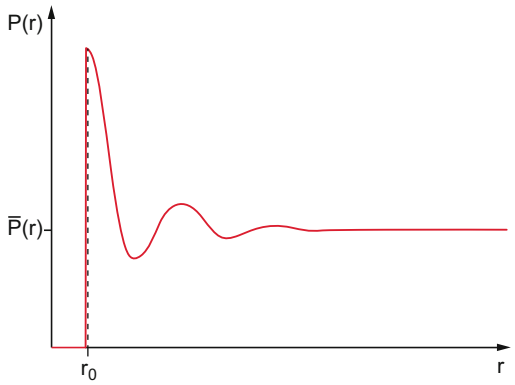

Figure 6.4 Probability $P(r)$ that an atom A_1 in a liquid has the distance r to an arbitrary other atom A_2

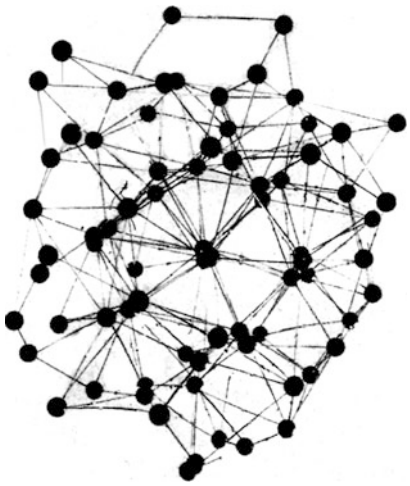

Figure 6.5 Atomic model of a liquid. The balls are connected with each other by strings. The model illustrates the free mobility of each atom

and the atoms can move freely. They form a gas that fills the total accessible volume. The interaction energy is only noticeable during collisions of the atoms with each other.

The mean distance $\langle r \rangle$ between the atoms or molecules and therefore also the density $\varrho = M/V$ of the gas with total mass M depends on the volume V which is accessible to the $N = M/m$ molecules with mass m. At normal pressure $p = 1$ bar the density of the gas is about three orders of magnitude smaller than that of solids or liquids.

Examples

The density of air at $p = 1$ bar and $T = 300\,\mathrm{K} (\approx 20\,^\circ\mathrm{C})$ is $\varrho = 1.24\,\mathrm{kg/m^3}$, while the density of water is about $10^3\,\mathrm{kg/m^3}$ and that of lead is $11.3 \cdot 10^3\,\mathrm{kg/m^3}$. ◀

The considerations above show that the aggregation state of material depends on the ratio $\langle E_{\mathrm{kin}} \rangle / E_{\mathrm{p}}$ and therefore on the temperature and on the binding energy of the atoms or molecules of the body.

We will now discuss the most important characteristic features of the different aggregation states in a phenomenological manner. The more detailed treatment is given in Vol. 3.

6.2 Deformable Solid Bodies

External forces can change the shape of solid bodies. If the body returns to its original shape after the exposure to the external forces we call it elastic. For a plastic body the deformation remains.

6.2.1 Hooke's Law

If a pulling force acts onto the end face of an elastic rod with length L and cross section A, which is hold tight at the other end $x = 0$ (Fig. 6.6) the length L is prolonged by ΔL. The linear relation between the magnitude $F = |\boldsymbol{F}|$ of the force and the prolongation ΔL

$$F = E \cdot A \cdot \Delta L / L \tag{6.2}$$

is called *Hooke's law*, which is valid for sufficiently small relative length changes $\Delta L/L$. The proportional factor E is the *elastic modulus* with the dimension $\mathrm{N/m^2}$. For technical applications often the dimension $\mathrm{kN/mm^2} = 10^9\,\mathrm{N/m^2}$ is used. Table 6.1 gives numerical values for some materials.

For materials with a large elastic modulus E one needs a large force to achieve a given relative change of length $\Delta L/L$. With other words: Materials with a large value of E show for a given force a small relative length change.

Introducing the tensile stress (= pulling force/cross section A)

$$\sigma = F/A$$

and the relative stretch or strain $\varepsilon = \Delta L/L$ Hooke's law can be written in the clearer form

$$\sigma = E \cdot \varepsilon\ . \tag{6.2a}$$

For sufficiently small relative stretches ε, tensile stress and strain are proportional. In this proportional range the distances between neighboring atoms vary only within a small range around r_0 (Fig. 6.1) where the interatomic force $F(r) = a \cdot r$ is approximately a linear function of the distance r and the potential energy $E_\mathrm{p}(r)$ can be approximated by a parabola.

Note: This linear relation is only an approximation for small values of ε. For larger ε nonlinear forces appear that cannot be neglected.

Expanding $E_\mathrm{p}(r)$ into a Taylor series around the equilibrium position r_0

$$E_\mathrm{p}(r) = \sum_{n=0}^{\infty} \frac{(r-r_0)^n}{n!} \left(\frac{\partial^n E_\mathrm{p}}{\partial r^n}\right)_{r=r_0} \tag{6.3a}$$

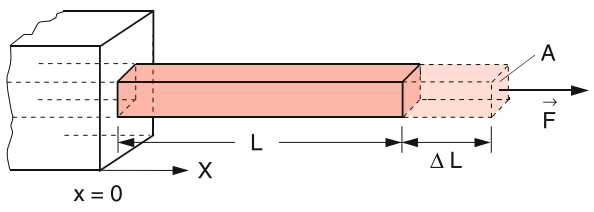

Figure 6.6 A rod fixed at $x = 0$ expands under the action of a force $\vec{F}$ by $\Delta L = F \cdot L/(E \cdot A)$

Table 6.1 Elastic constants of some solid materials. E = elastic modulus; G = modulus of shear; K = compressibility modulus; μ = inverse contraction number = Poisson number; [6.1]

Material	E [10^9 N/m^2]	G [10^9 N/m^2]	K [10^9 N/m^2]	μ
Aluminium	71	26	74	0.34
Cast iron	64–181	25–71	48–137	0.28
Ferrite steel	108–212	42–83	82–161	0.28
Stainless steel	200	80	167	0.3
Copper	125	46	139	0.35
Tungsten	407	158	323	0.29
Lead	19	7	53	0.44
Fused silica	75	32	38	0.17
Water ice (−4 °C)	10	3.6	9	0.33

and choosing the minimum of $E_\mathrm{p}(r)$ as $E_\mathrm{p}(r_0) = 0$, the first two members of the Taylor series (6.3a) vanish because also $\partial E_\mathrm{p}/\partial r|_{r=0} = 0$. This reduces (6.3a) to

$$E_\mathrm{p}(r) = \frac{1}{2}(r-r_0)^2 \left(\frac{\partial^2 E_\mathrm{p}}{\partial r^2}\right)_{r=r_0} + \frac{1}{6}(r-r_0)^3 \left(\frac{\partial^3 E_\mathrm{p}}{\partial r^3}\right)_{r=r_0} + \ldots\ . \tag{6.3b}$$

For small elongations $(r - r_0)$ all higher order terms with powers $n \geq 3$ can be neglected and (6.3b) gives for the force $\boldsymbol{F} = -\mathbf{grad}\ E_\mathrm{p}$ the linear relation of Hooke's law. For larger elongations, however, the higher order terms can no longer be neglected and must be taken into account.

Surpassing the linear range at the point P in Fig. 6.7 the relative stretch ε increases faster than the tensile stress σ (Fig. 6.7). The material is still elastic until the point F, i.e. it returns nearly to its initial length after the stress is released. Above the yield point F, internal shifts of atomic layers (lattice planes) occur (Fig. 6.8). The body becomes malleable and the plastic flow starts. Permanent changes of shape remain after the termination of the external force. While for the elastic stretch the distances r between the atoms increases linearly by $\Delta r \approx (\Delta L/L) r_0$ the

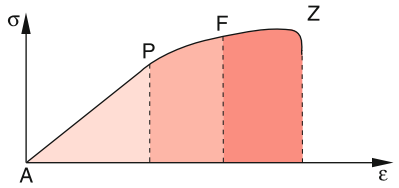

Figure 6.7 Relative length change ε of a body caused by an external tensile force σ. Beyond the point P the linear elongation changes to a nonlinear one. The point F marks the yield point, the point Z the tear point

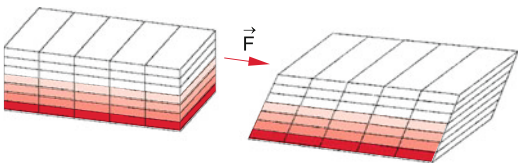

Figure 6.8 Model of plastic flow of a solid explained by shift of atomic planes

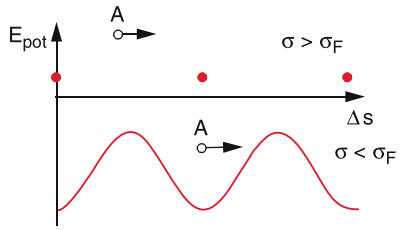

Figure 6.9 Atomic model of elastic expansion of a solid. The atom *A* moves in the potential well but does not leave it

flow process can be achieved by a shift of the atomic planes against each other, as illustrated in Fig. 6.8.

This can be made clear by Fig. 6.9 which shows the potential energy of an atom *A* in an atomic plane. For small length changes all atoms remain within their potential well. For larger changes the atomic plane is shifted against the adjacent plane. The atom can move from one minimum into the next only if the external pulling force is sufficiently large to lift all atoms of this plane over the potential hills. Since such a shift changes the distance between atoms only slightly, the minima in Fig. 6.9 are much shallower than the minimum of the potential energy between two atoms in Fig. 6.1. The barrier height and the modulation period of $E_p(\Delta L)$ depends for an anisotropic crystal on the direction of the pulling force relative to the crystal axes.

In a real crystal lattice, defects and dislocations are present which influence the flow process and can increase or decrease the renitence against stretches and shifts of crystal planes against each other.

6.2.2 Transverse Contraction

When a rod is stretched by an external pulling force, not only the length L in the direction of the force is prolonged but also the cross section decreases (Fig. 6.10). For a rod with length L and quadratic cross section d^2 the change ΔV of its volume V under a length stretch $\Delta L > 0$ and $\Delta d < 0$ is

$$\begin{aligned}\Delta V &= (d+\Delta d)^2 \cdot (L+\Delta L) - d^2 L \\ &= d^2 \Delta L + 2L \cdot d\Delta d \\ &\quad + \left(L\Delta d^2 + 2d\Delta d\Delta L + \Delta L \Delta d^2\right) .\end{aligned}$$

For small deformations ($\Delta L \ll L$ and $\Delta d \ll d$), the terms in the bracket can be neglected, because they converge quadratic or even cubic towards zero for $\Delta L \to 0$. This reduces the above equation to

$$\frac{\Delta V}{V} \approx \frac{\Delta L}{L} + 2\frac{\Delta d}{d} . \tag{6.4}$$

The quantity

$$\mu \overset{\text{Def}}{=} -\frac{\Delta d}{d} \Big/ \frac{\Delta L}{L} \tag{6.5}$$

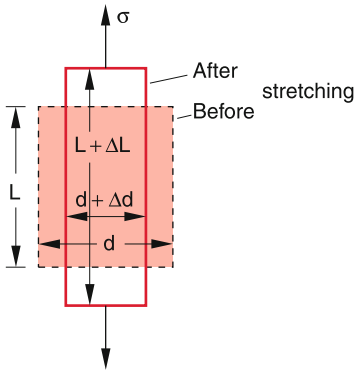

Figure 6.10 Transverse contraction under the influence of longitudinal tensile stress

is called the *transverse contraction ratio* because it is the ratio of transverse contraction to longitudinal elongation. The relative volume change is then expressed as

$$\frac{\Delta V}{V} = \frac{\Delta L}{L}\left(1 + \frac{2\Delta d/d}{\Delta L/L}\right) = \varepsilon\,(1-2\mu) . \tag{6.6a}$$

Since a pulling force increases the volume ($\Delta V > 0$), we obtain for μ the condition $\mu < 0.5$. According to Hooke's law (6.2a) is $\Delta L/L = \sigma/E$. Inserting this into (6.6a) gives

$$\frac{\Delta V}{V} = \frac{\sigma}{E}\,(1-2\mu) . \tag{6.6b}$$

If a pressure instead of a tensile stress is exerted onto the end faces of a rod, ΔL and ΔV become negative but Δd positive because the rod is compressed in the length direction which causes an increase of its cross section. The resulting relative volume change can be obtained from (6.6b) when σ is replaced by the pressure p.

In both cases is $\mu > 0$ because for the pulling force is $\Delta L > 0$ and $\Delta d < 0$ while in case of a pressure is $\Delta L < 0$ and $\Delta d > 0$, which means that the ratio in the bracket in (6.6a) does not change its sign.

If the body is exerted to an isotropic pressure $p = -\sigma$, which acts onto all sides of the body, the resulting volume change can be obtained by the following consideration.

The pressure acting on the end faces d^2 decreases the length L by $\Delta L = -L \cdot p/E$, the pressure acting on the sides decreases the transverse edge length by $\Delta d = -d \cdot p/E$. However, because of the transverse action on the elongation this transverse contraction increases the length by $\Delta L = +\mu \cdot L \cdot p/E$. Taking both effects in account the length L under the action of a uniform pressure p changes by

$$\Delta L = -\,(L \cdot p/E)\,(1-2\mu) . \tag{6.7}$$

In a similar way the transverse dimension d is changed by

$$\Delta d = -\,(d \cdot p/E)\,(1-2\mu) .$$

Since $\Delta L \ll L$ and $\Delta d \ll d$ the higher order terms in the expansion of $\Delta V/V = \Delta L/L + 2\Delta d/d$ can be neglected and we obtain

$$\frac{\Delta V}{V} = \frac{\Delta L}{L} + \frac{2\Delta d}{d} = -\frac{3p}{E}(1-2\mu) \ . \tag{6.8}$$

Introducing the compressibility modulus K by the equation

$$p = -K \cdot \frac{\Delta V}{V} \tag{6.9}$$

and the coefficient of compressibility $\kappa = 1/K$, Eq. 6.8 can be written as

$$\kappa = \frac{1}{K} = \frac{3}{E}(1-2\mu) \ . \tag{6.10}$$

This gives the relations between compressibility modulus K, coefficient of compressibility κ, elastic modulus E and transverse contraction number (Poisson number) μ.

6.2.3 Shearing and Torsion Module

A shear force $\boldsymbol{F}$ is a force, which acts on a body parallel to a plane surface A (Fig. 6.11). The shearing stress

$$\tau = \boldsymbol{F}/A$$

is the tangential shearing force $\boldsymbol{F}$ per unit surface area A. The result of the action of a shearing stress is a tilt of the axis of the cuboid in Fig. 6.11 by an angle α. For sufficiently small tilting angles α, the experiments prove that the tilting angle α is proportional to the applied shearing stress.

$$T = G \cdot \alpha \ . \tag{6.11}$$

The constant G is called *modulus of shear* (or modulus of torsion).

Since the restoring forces under deformations of an elastic body are due to interatomic forces, all elastic constants E, μ, K and G must be related to each other.

As can be proved [6.2] for isotropic bodies the following relation holds:

$$E/2G = 1 + \mu \ . \tag{6.12a}$$

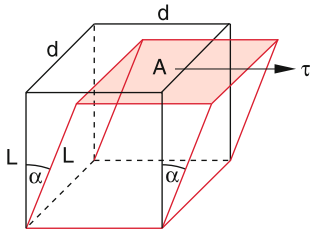

Figure 6.11 Shearing of a cube under the action of shearing stress τ

Rearrangement of (6.10) yields

$$E/3K = 1 - 2\mu \ . \tag{6.12b}$$

The division of (6.12a) by (6.12b) gives

$$2G/3K = \frac{1-2\mu}{1+\mu} \ . \tag{6.12c}$$

Example

Torsion of a wire: We assume a force $\boldsymbol{F}$ that acts tangential on a cylinder with radius R and length L and which causes a torsion of the cylinder (Fig. 6.12). We subdivide the cylinder in thin radial cylindrical shucks between the radii r and $r+\mathrm{d}r$ and in axial strips with the angular width $\delta\varphi$. If the upper end of the cylinder twists under the action of a torsional force $\boldsymbol{F}$ by the angle φ the prismatic column marked in red in Fig. 6.12 experiences a shear by the angle α. For $r \cdot \varphi \ll L$ one finds $\alpha = r \cdot \varphi/L$.

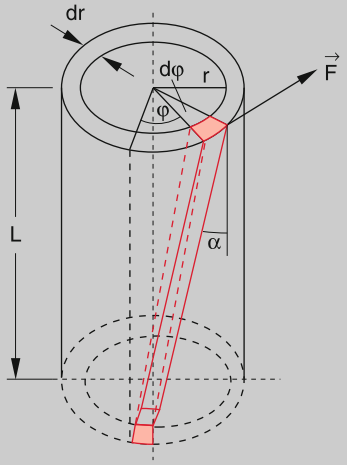

Figure 6.12 Torsion of a circular cylinder

The shearing stress necessary to achieve this torsion is according to (6.11)

$$\tau = G \cdot r \cdot \varphi/L \ .$$

Since all surface elements of the upper annulus with the area $2\pi r \cdot \mathrm{d}r$ are twisted by the same angle φ against their position for $\tau = 0$ the amount of the force $\mathrm{d}F$ necessary for the shear of the whole cylindrical shuck is

$$\mathrm{d}F = \tau \cdot 2\pi r \cdot \mathrm{d}r = 2\pi r^2 \cdot \mathrm{d}r \cdot \varphi \cdot g/L$$

and the corresponding torque is

$$\mathrm{d}D = r \cdot \mathrm{d}F = 2\pi \cdot r^3 \cdot \mathrm{d}r \cdot G \cdot \varphi/L \ .$$

The torsion of the whole cylinder with radius R by the angle φ is then accomplished by the torque

$$D = \frac{2\pi G\varphi}{L}\int_0^R r^3 \mathrm{d}r = \frac{\pi}{2}G\frac{R^4}{L}\cdot\varphi\ . \qquad (6.13)$$

At equilibrium, the retro-driving torque, due to the elastic twist of the cylinder, must be equal to the external torque. This gives for the retro-driving torque

$$D^* = -D_\mathrm{r}\cdot\varphi \quad \text{with } D_\mathrm{r} = \frac{\pi}{2}G\frac{R^4}{L}\ . \qquad (6.14)$$

The constant D_r, which depends on the shear modulus G and gives the torque per unit angle, is called *restoring torque*.

If a body with the moment of inertia I with respect to the symmetry axis, is fixed to the lower end of a wire this torsional pendulum performs rotary oscillations after the wire has been twisted (see Sect. 5.6.2) with the oscillation period

$$T = 2\pi\sqrt{\frac{I}{D_\mathrm{r}}} = \frac{2\pi}{R^2}\sqrt{\frac{2L\cdot I}{\pi\cdot G}}\ . \qquad (6.15)$$

Such a torsional pendulum is a very sensitive device for measurements of small torques. Examples are the Eötvös's torsional pendulum for the measurement of Newton's gravitational constant (see Sect. 2.9.6), Coulomb's torsional pendulum for the measurement of the electric force between charges (Vol. 2, Chap. 1) and many modifications of Galvanometers for the measurement of small electric currents (Vol. 2, Chap. 2). ◀

6.2.4 Bending of a Balk

For technical constructions (buildings, bridges, etc.) the bending of balks under the influence of suspended weights represents an important problem and can decide about the stability of the construction. We will illustrate the problem with a simple example, where a rod with a rectangular cross section $A = d\cdot b$ is clamped at one end while a force acts on the other free end (Fig. 6.13). The calculation of such bending for arbitrary bodies is very complicated and can be accomplished only numerically.

If a rectangular rod with cross section $A = d\cdot b$ is clamped at $x = 0$ and a force F_0 is acting in the $-z$-direction on the other end at $x = L$, the bending of the rod can be approximately described by approximating a short curved section of the rod by a circle. When the central dashed curve in Fig. 6.14 has the radius of curvature r, the length of the upper edge of the rod section is $(r + d/2)\varphi$, that of the lower edge is $(r - d/2)\varphi$.

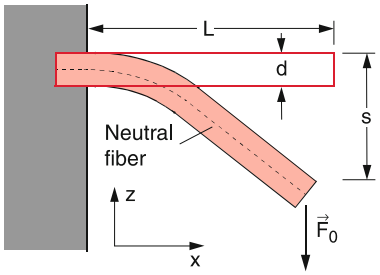

Figure 6.13 Bending of a rod which is clamped at one end

While the length of the central curve does not change by the bending (neutral filament) the length $\ell(z)$ of a layer in the upper half of the rod ($z > 0$) increases by the amount

$$\Delta\ell(z) = z\cdot\varphi = z\cdot\ell/r\ .$$

A corresponding layer in the lower half ($z < 0$) is shortened by this amount. In order to achieve such an increase of the length ℓ a pulling force per unit cross section (tensile stress)

$$\sigma = E\cdot\Delta\ell/\ell = z\cdot E/r$$

has to be applied, while for the layer in the lower half ($z < 0$) a corresponding pressure

$$p = -\sigma = -|z|\cdot E/r$$

is necessary. The force on a rectangular element with width b, heights $\mathrm{d}z$ and distance z from the neutral filament at $z = 0$ is then

$$\mathrm{d}F = \sigma b\mathrm{d}z = \frac{bE}{r}z\mathrm{d}z\ . \qquad (6.16a)$$

The force causes a torque

$$\mathrm{d}D_y = \frac{bE}{r}z^2\mathrm{d}z \qquad (6.16b)$$

in the y-direction.

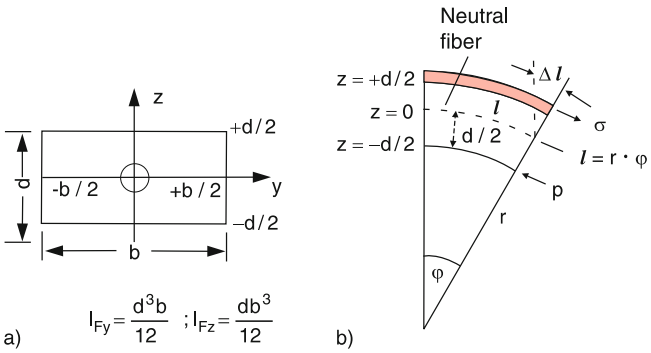

Figure 6.14 **a** Definition of the neutral filament at $z = 0$. **b** Illustration of (6.17)

Integration of this infinitesimal torque dD_y over the total height d of the rod gives

$$D_y = \frac{bE}{r}\int_{-d/2}^{+d/2} z^2 dz = \frac{Ed^3 b}{12r} . \qquad (6.17)$$

This torque is caused by the vertical force F_0 at the end $x = L$ of the rod. On the other hand the torque induced by the force F_0 on a selected part of the rod at the position x is

$$D_y = F_0(L-x) \quad \text{with} \quad F_0 = |\boldsymbol{F_0}| . \qquad (6.18)$$

The equilibrium position of the bent rod is determined by the condition that the restoring torque of the elastic material (6.17) must just compensate the torque (6.18). This yields the curvature $1/r$ of the rod at the distance x from the fixed end at $x = 0$:

$$1/r = -\frac{12F_0}{Ed^3 b}\cdot(L-x) . \qquad (6.19)$$

The neutral filament which is without a force the horizontal straight line $z = 0$, becomes the bent curve $z = z(x)$. As is shown in books on differential geometry the relation between the curvature $1/r$ and the function $z = z(x)$ is

$$1/r = \frac{z''(x)}{[1+z'(x)^2]^{3/2}} ,$$

where $z'(x) = dz/dx$ and $z''(x) = d^2z/dx^2$. For small curvatures is $z'(x) \ll 1$ and therefore $1/r$ can be approximated by $1/r \approx z''(x)$. Integration of the equation

$$z''(x) = a\cdot(L-x) \quad \text{with } a = -12F_0/Ed^3 b$$

derived from (6.17) and (6.18), gives with the boundary conditions $z(0) = 0$ and $z'(0) = 0$ the function of the neutral filament of the strained rod

$$z(x) = \frac{a}{2}Lx^2 - \frac{a}{6}x^3 \quad \text{with } a < 0 .$$

The free end of the rod at $x = L$ bends by

$$s_{\max} = z(L) = -4\frac{L^3}{E\cdot d^3 b}F_0 \qquad (6.20)$$

compared to $z(L) = 0$ for the straight rod. The bend of the rod $s = z(L)$ is also called *pitch of deflection sag*.

The bend of a rectangular rod with length L and thickness d is proportional to L^3 and to $1/d^3$.

For $x = 0$ (at the clamped end of the rod) the curvature $1/r = z''(0) = a\cdot L$ becomes maximum. The tensile stress at the upper edge of the rod ($z = +d/2$) is

$$\sigma_{\max} = \frac{E\cdot d}{2r} = \frac{12F_0\cdot L}{2d^2 b} . \qquad (6.21)$$

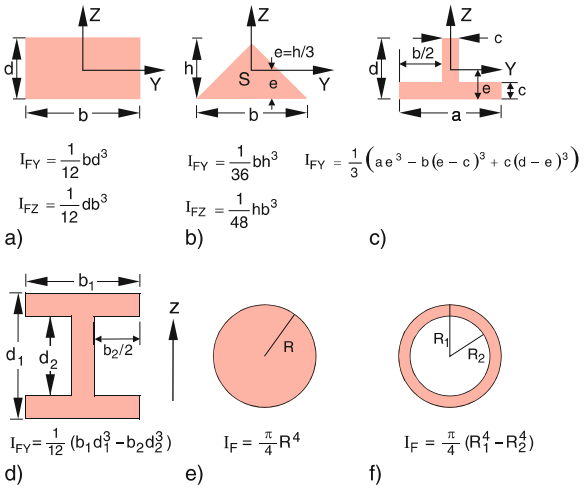

Figure 6.15 Geometrical moments of inertia for some selected cross sections. I_{Fy}: bending about the y-axis; I_{Fz}: about the z-axis

As soon as $\sigma_{\max}$ exceeds the fracture stress of the rod material, the rod starts to notch at the upper edge at $z = +d/2$ and $x = 0$ and the rod cracks.

Remark. The bend of rods with arbitrary cross section $A = \int dy dz$ can be treated in a similar way if one introduces the *geometrical moment of inertia* (*second moment of area*)

$$I_F \overset{\text{Def}}{=} \iint z^2 dy dz , \qquad (6.22a)$$

where z is the direction of the acting force $\boldsymbol{F}$. For the rod with rectangular cross section $A = d\cdot b$ (Fig. 6.15b) we get

$$I_F = \int_{z=-d/2}^{+d/2}\int_{y=-b/2}^{+b/2} z^2 dy dz = \frac{1}{12}d^3 b . \qquad (6.22b)$$

The maximum deflection $s_{\max}$ (pitch of deflection sag) is, in accordance with (6.20),

$$s_{\max} = -\frac{L^3}{3E\cdot I_F}F . \qquad (6.23)$$

For a rod with circular cross section (radius R) (Fig. 6.15e) we get

$$I_F = \frac{1}{4}\pi R^4$$

and therefore

$$s_{\max} = -\frac{4L^3}{3\pi E R^4}F . \qquad (6.24)$$

For a double T-beam (Fig. 6.15d) is

$$I_F = \frac{1}{12}\left(b_1 d_1^3 - b_2 d_2^3\right) . \qquad (6.25)$$

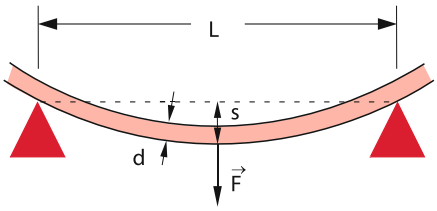

Figure 6.16 Bending of a rod, which is clamped at both ends

A beam with length L, supported on both ends by fixed bearings, suffers by a force F acting at the midpoint $x = L/2$ (Fig. 6.16) the maximum sag

$$s_{\max} = -\frac{1}{4E}\frac{L^3}{d^3 b} \cdot F \,. \tag{6.26}$$

Note, that here the sag is smaller by a factor 16! compared to the rod which is fixed only at one end (because of the L^3 dependence). The force is now distributed onto the two halves of the rod with $L/2$ each.

6.2.5 Elastic Hysteresis; Energy of Deformation

When a rod without deformation is exposed to an external tensile stress σ between the end faces the relative stretch $\varepsilon = \Delta L/L$ follows the curve OA in Fig. 6.17. For small values of ε the curve $\sigma(\varepsilon)$ is linear until a point is reached where the deformation is no longer reversible and $\sigma(\varepsilon)$ rises slower than linear. The point A in Fig. 6.17 is already in the irreversible region. This means that the curve $\sigma(\varepsilon)$ does not return on the same curve when the stress is released but arrives at the point B for $\sigma = 0$. This phenomenon is called *elastic hysteresis*, because the stress-free state of the body depends on its past history (the Greek word *hysteresis* means: lagging behind i.e. the length change lags behind the applied stress).

When the body in the state B is exposed to an external pressure $p = -\sigma$ onto the two end faces the curve $\sigma(\varepsilon)$ reaches the point C where it is also nonlinear. Releasing the pressure ε does not become zero for $\sigma = 0$ but arrives at the point D in Fig. 6.17, which corresponds in the atomic model of Fig. 6.1 to an interatomic distance $r < r_0$.

Under a periodic change between stretch and compression the function $\sigma(\varepsilon)$ passes through the closed loop ABCDA, which is called the elastic hysteresis loop. During a roundtrip one has to expend work against the interatomic forces because the interatomic distances r are periodically increased (stress) and decreased (compression). When the length L of a quadratic rod

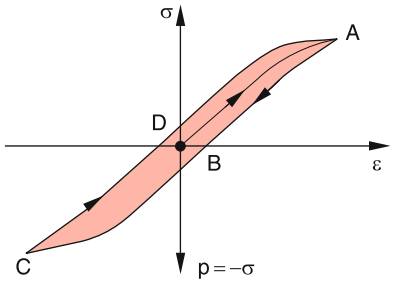

Figure 6.17 Mechanical hysteresis curve

with cross section A increases by ΔL the necessary work is

$$\begin{aligned} W &= \int_0^{\Delta L} F \mathrm{d}L = \int_0^{\Delta L} A \cdot \sigma \mathrm{d}L \\ &= \int_0^{\varepsilon} A\sigma \cdot L \mathrm{d}\varepsilon = V \cdot \int_0^{\varepsilon} \sigma \mathrm{d}\varepsilon \,. \end{aligned} \tag{6.27}$$

The integral $\int \sigma \cdot d\varepsilon$ represents the work per unit volume, necessary for the relative length change ε.

In the region where Hooke's law is valid (linear region of $\sigma(\varepsilon)$ is $\sigma = E \cdot \varepsilon$ and the work for the elastic length change ΔL

$$W_{\text{elast}} = \tfrac{1}{2} E \cdot V \cdot \varepsilon^2 \,. \tag{6.28}$$

Returning to the original stress-free state this energy is again released. The hysteresis curve simplifies to a straight line through the origin $\sigma = \varepsilon = 0$.

Example

Elongation and compression of an elastic spiral spring during the oscillation of a mass m that hangs on the spring. During the oscillation with small amplitude with the linear region of Hooke's law, the potential energy of the spring and the kinetic energy of the mass m are periodically converted into each other (see Example 2 in Sect. 2.7.4 and Sect. 11.6). The total energy, however, is always conserved. ◀

This is no longer true for the nonlinear part of the curve $\sigma(\varepsilon)$ in Fig. 6.17. Here the work $\int \sigma \cdot \mathrm{d}\varepsilon$ has to be put into the system in order to proceed from the point O to the point A. This work is equal to the area under the curve OA. However, after releasing the tensile stress, only the work $\int \sigma \cdot \mathrm{d}\varepsilon$ that equals the area under the curve AB can be regained. The rest is converted into thermal energy, due to the non-elastic deformation of the body.

Altogether the net work per unit volume, put into the system during a roundtrip along the curve ABCDA, is given by the area enclosed by this hysteresis curve in Fig. 6.17.

Table 6.2 Hardness scale according to Mohs

Selected materials as measurement standards		Examples	
1. Tallow	6. Feldspar	Aluminium	2.3–2.9
2. Gypsum	7. Quartz	Lead	1.5
3. Calcite	8. Topaz	Chromium	8
4. Fluorite	9. Corundum	Iron	3.5–4.5
5. Apatite	10. Diamond	Graphite	1
		Tungsten	7

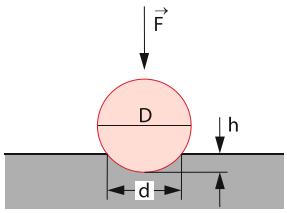

Figure 6.18 Hardness test according to *Brinell*

6.2.6 The Hardness of a Solid Body

The hardness of a body is a measure for the resistance, which the body sets against a penetration of another body. Depending on the measuring technique, there are some slightly different hardness values. The scratch-method introduced 1820 by Mohs, defines a body A as harder than a body B if it is possible to scratch B with A. The *hardness scale of Mohr* is based on this definition. Here the hardness scale is divided into 10 degrees of hardness based on 10 selected minerals, listed in Tab. 6.2.

The scratch method measures in fact mainly the hardness of the surface. This surface hardness is of particular importance for technical applications, because the attrition of tools or of axes and bearings depends on the surface hardness. Therefore, several techniques have been developed for the enhancement of the surface hardness. One example is the transformation of the surface layers of a crystalline solid into an amorphous state by irradiation with a powerful laser. Another example is the cover of solid tools, e.g. drills or steel mills, with a thin layer of a hard material such as carbon-nitride NC or titanium Ti.

For measuring the hardness of a body, often a technique is used which had been proposed by *Brinell* in 1900. Here a hardened steel ball with diameter D is pressed vertically with a constant force $F = a \cdot D^2$ into the sample (Fig. 6.18). The diameter d of the resulting circular notch in the sample gives the penetration depth, which is a measure for the *Brinell-hardness*.

6.3 Static Liquids; Hydrostatics

In order to achieve a change of the shape of solid bodies substantial forces are required, even if the volume of the body does not change (for example for a shear or a torsion). Although similarly large forces are necessary for a compression of liquids, a mere deformation of liquids at constant volume requires only very small forces and are merely caused by friction or surface effects.

At first we will discuss the simplified model of an ideal liquid, where surface effects and friction are neglected. For the static case of a liquid at rest, friction does not occur anyway. Surface effects will be treated in Sect. 6.4 and the influence of friction for streaming liquids is discussed in Chap. 8.

6.3.1 Free Displacement and Surfaces of Liquids

For ideal liquids without friction, there is no force necessary to deform a given liquid volume. In the atomic model this means: While in solid bodies the atoms can vibrate around fixed equilibrium positions, which do not change much under moderate external forces, the atoms or molecules in liquids can freely move around within the given liquid volume, determined by the solid container (Fig. 6.5). In the macroscopic model this free movement can be expressed by the statement:

> The shear modulus of an ideal liquid is zero.

This implies that at the surface of an ideal liquid no tangential forces can be present, because they would immediately deform the liquid until the forces disappear and a minimum energy is achieved. This force-free condition represents a stable state of the liquid.

The surface of an ideal liquid is always perpendicular to the total external force.

Examples

1. If only gravity acts onto a liquid, the surface of the liquid forms always a horizontal plane (Fig. 6.19a)
2. The surface of a liquid in a cylinder which rotates about a vertical axis (Fig. 6.19b) forms a surface where the total force composed of gravity $m \cdot g$ in the $-z$-direction and centrifugal force $m\omega^2 \cdot r$ in the radial direction points perpendicular to the surface. The slope of the intersection curve $z(r)$ of the surface at the point A in Fig. 6.19b is

$$\tan\alpha = \frac{m\omega^2 r}{m \cdot g} = \frac{\omega^2 r}{g} .$$

On the other hand the slope of the curve $z(r)$ is given by $\tan\alpha = \mathrm{d}z/\mathrm{d}r$. Integration yields

$$z(r) = \frac{\omega^2}{g} \int r\mathrm{d}r = \frac{\omega^2}{2g} r^2 + C .$$

For $z(0) = z_0$ is $C = z_0$ and we get

$$z(r) = \frac{\omega^2}{2g} r^2 + z_0 \,. \qquad (6.29)$$

The surface forms a rotational paraboloid with its axis coincident with the rotation axis.

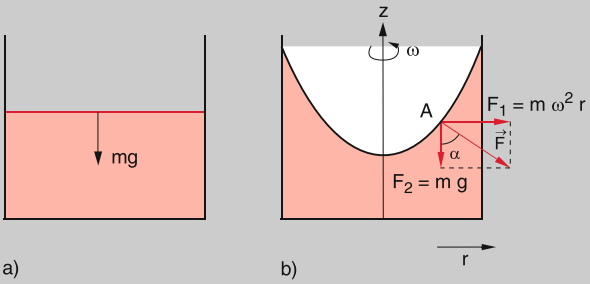

Figure 6.19 **a** Horizontal liquid surface in a container at rest. **b** Surface as rotational paraboloid in a rotating container ◀

6.3.2 Static Pressure in a Liquid

Any external force acts only vertically on the surface of a liquid. If a container with a liquid is closed by a movable piston with surface A, onto which a vertical force F acts (Fig. 6.20) we define the pressure onto the liquid as

$$p = F/A, \quad \text{with} \quad F = |\boldsymbol{F}| \,.$$

6.3.2.1 Forces onto a Liquid Volume Element

We consider an arbitrary cuboid volume element $dV = dx{\cdot}dy{\cdot}dz$ inside the liquid (Fig. 6.21). We assume that a pressure p acts in x-direction onto the left side $dy \cdot dz$ of the cuboid. Then a pressure

$$p + \partial p/\partial x \cdot dx$$

acts onto the opposite side. The resulting force on the volume element is then

$$F_x = p \cdot dydz - \left(p + \frac{\partial p}{\partial x} dx\right) dydz = -\frac{\partial p}{\partial x} dV \,.$$

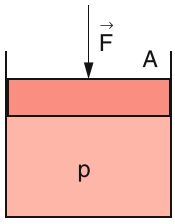

Figure 6.20 The force F, acting on a piston with area A generates a pressure $p = F/A$ in the liquid

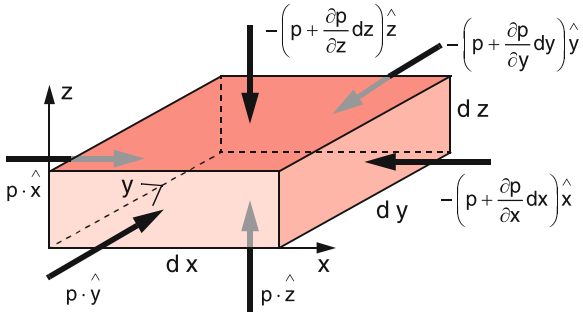

Figure 6.21 Relation between the pressure inside a volume element dV and the forces acting onto the sides of dV

In an analogous way we obtain the force components in the other directions

$$F_y = -\frac{\partial p}{\partial y} dV \quad \text{and} \quad F_z = -\frac{\partial p}{\partial z} dV \,.$$

We can condense these three equations into the vector equation

$$\boldsymbol{F} = -\mathbf{grad}\, p \cdot dV \,. \qquad (6.30)$$

Because of the free mobility of any volume element inside the liquid the total force onto a volume element at rest must be zero. This implies that $\mathbf{grad}\, p = \mathbf{0}$.

> The pressure inside the whole liquid is constant as long as no unisotropic forces act onto the liquid.

For a static liquid the same pressure acts onto all surface elements of the container!

This can be experimentally demonstrated by the simple device shown in Fig. 6.22. A spherical container with small holes in several directions of the x-y-plane is filled with dyed water and placed above a blotting paper in the plane $z = 0$. When a piston

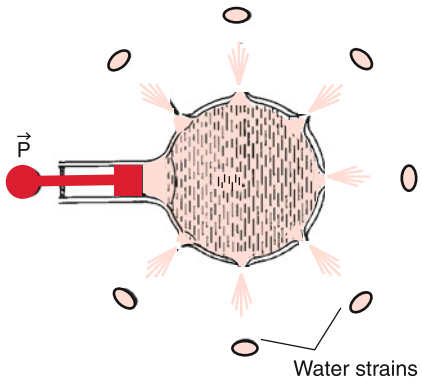

Figure 6.22 Demonstration of the isotropic pressure in a liquid. When the piston is moved the pressure p increases and the dyed water splashes through holes onto a white paper below the device, where the spots form a circle around the center, indication equal pressure

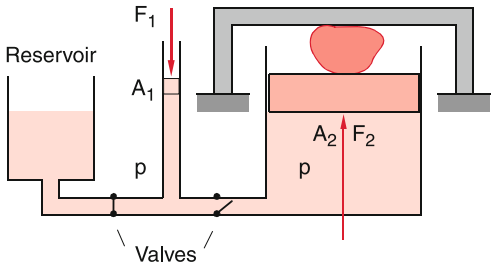

Figure 6.23 Hydraulic press (forces are drawn not to scale)

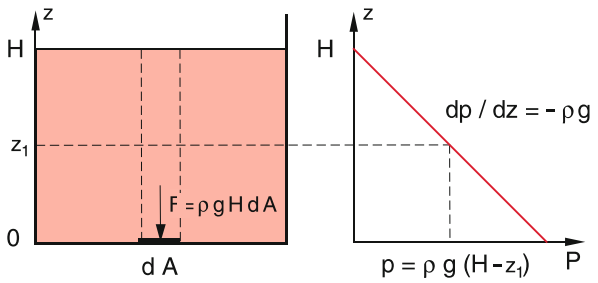

Figure 6.24 Pressure $p(z)$ in an incompressible liquid in the gravity field of the earth, as a function of height z above ground

is pressed to increase the pressure the water streams out of the holes and all water filaments follow projectile trajectories. Their points of impact on the blotting paper in the plane $z = 0$ form a circle which proves that they all had the same initial velocity, i.e. they stream out driven by the same pressure.

Application: Hydraulic press (Fig. 6.23)
Two cylinders with cross sections A_1 and $A_2 \gg A_1$ that are connected with each other, and are therefore at the same pressure p, are filled with a liquid. Applying the force $F_1 = p \cdot A_1$ on a piston in the narrow cylinder causes a force $F_2 = pA_2 = (A_2/A_1) \cdot F_1 \gg F_1$ acting on a piston in the large cylinder which presses a sample against a fixed mounting. For demonstration experiments, large stones can be cracked by this device. For a displacement Δx_2 of the large piston, the small piston has to move by the much larger amount $\Delta x_1 = (A_2/A_1) \cdot \Delta x_1$, because the volume $\Delta V_2 = A_2 \cdot \Delta x_2 = \Delta V_1 = A_1 \cdot \Delta x_1$ transferred from the small to the large cylinder must be of course equal.

6.3.2.2 Hydrostatic Pressure

Taking into account that every volume element ΔV of a liquid has a weight $\varrho \cdot g \cdot \Delta V$ in the gravity field of the earth, even without external force a pressure onto the bottom of the container is present due to the weight of the liquid above the bottom. For a height $z = H$ of the liquid the hydrostatic pressure at the bottom with area A is with $\mathrm{d}V = A \cdot \mathrm{d}z$

$$p(z=0) = \int_0^H \frac{\varrho \cdot g \cdot A}{A} \mathrm{d}z = \varrho \cdot g \cdot H \,, \qquad (6.31)$$

if we assume that the density ϱ is independent of the pressure p.

For real liquids, there is a small change of ϱ with the pressure p. A measure for this dependence is the compressibility

$$\kappa \overset{\text{Def}}{=} -\frac{1}{V}\frac{\partial V}{\partial p} \,, \qquad (6.32)$$

which describes the relative volume change $\Delta V/V$ for a change Δp of the pressure.

For liquids κ is very small (for example for water is $\kappa = 5 \cdot 10^{-10}\,\mathrm{m^2/N}$). This shows that the density ϱ of a liquid changes only by a tiny amount with pressure and in most cases the density $\varrho(p) = \varrho_0$ can be assumed to be constant.

Then it follows from (6.31) for the pressure $p(z)$ in a liquid with total heights H (Fig. 6.24)

$$p(z) = \varrho \cdot g \cdot (H - z) \,.$$

The SI unit for the pressure is 1 Pascal $= 1\,\mathrm{Pa} = 1\,\mathrm{N/m^2}$, which corresponds to 10^{-5} bar.

Examples

1. A water column of 10 m heights causes a hydrostatic pressure of $p = \varrho \cdot g \cdot h = 9.81 \cdot 10^4\,\mathrm{Pa} = 0.981\,\mathrm{bar} = 1$ atmosphere. At an ocean depth of 10.000 m (Philippine rift) the hydrostatic pressure is $\approx 10^8\,\mathrm{Pa}$ (about 1000 atm). The total force onto the outer surface of a hollow steel sphere of an aquanaut with 3 m diameter is at this depth $F = 2.8 \cdot 10^9\,\mathrm{N}$.

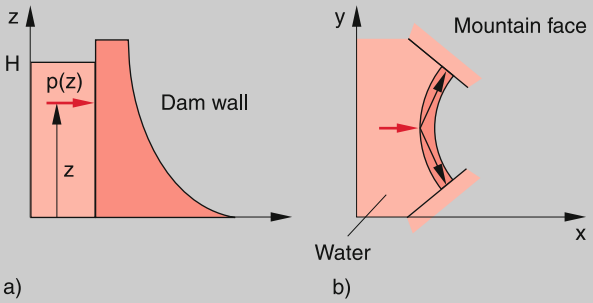

Figure 6.25 **a** Water pressure acting onto a dam wall; **b** Additional support by the mountain walls for a curved dam wall

2. The total force F onto the river dam with length L caused by the water with heights H can be obtained by integration over all contributions $F(z)\mathrm{d}z$ onto the surface elements $L \cdot \mathrm{d}z$ of the dam.

$$F = L \int p(z)\mathrm{d}z = \varrho \cdot g \cdot L \int (H - z)\mathrm{d}z$$
$$= \tfrac{1}{2}\varrho \cdot g \cdot L \cdot H^2$$

This force can be partly supported by choosing a curved dam where part of the force are balanced by the mountain walls (Fig. 6.25b). The thickness of the dam decreases with z in order to take into account the decreasing hydrostatic pressure (Fig. 6.25a). ◀

Figure 6.26 River dam of the river Eder, Germany. The bending of the dam towards the water side conducts part of the waterpressure against the mountain sides (see Sect. 6.3). With kind permission of Cramers Kunstverlag, Dortmund

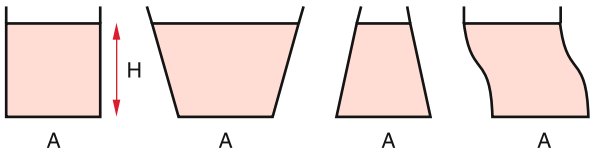

Figure 6.27 Hydrostatic paradoxon. The pressure onto the bottom is equal for all containers filled up to the same height H

Equation 6.31 tells us that the pressure p at the upper surface of a liquid volume element $\Delta V = A \cdot \Delta h$ with height Δh is smaller than at the bottom of this element by the amount $\varrho \cdot g \cdot \Delta h$. This results in an upwards force $F = A \cdot \varrho \cdot g \cdot \Delta h$, which is just compensated by the weight $G = M \cdot g = \varrho \cdot g \cdot \Delta V = \varrho \cdot g \cdot A \cdot \Delta h$ of the volume element. The total force on an arbitrary volume element ΔV inside a homogeneous liquid in a homogeneous gravity force field is therefore zero.

Since the hydrostatic pressure at the bottom of a liquid container depends only on the height H of the liquid but not on the shape of the container, the pressure at the bottom is identical for all four containers shown in Fig. 6.27, although the total mass of the liquid and therefore also its weight is different. This *hydrostatic paradox* leads to the following astonishing but true fact: When a hollow cube with a volume 1 m^3 is filled completely with water, the hydrostatic pressure at the bottom is 0.1 bar. If now a thin tube with 1 cm^2 cross section but 10 m height is put through a small hole in the top wall of the cube and filled with water the pressure in the cube rises to 1 bar. Although the additional mass of water is only 10^{-3} of the water in the cube the pressure rises by a factor of 10.

6.3.3 Buoyancy and Floatage

If we immerse a cuboid with basic area A and volume $V = A \cdot \Delta h$ into a liquid with density ϱ_L the pressure difference between bottom and top surface is (Fig. 6.28)

$$\Delta p = \varrho_L \cdot g \cdot \Delta h \, .$$

This results in an upwards directed buoyancy force

$$F_B = \varrho_L \cdot g \cdot A \cdot \Delta h = -G_L \, ,$$

which is equal to the weight G_L of the liquid displaced by the body, but has the opposite direction.

This can be formulated as *Archimedes' Principle*:

> A body immersed in a liquid looses seemingly as much of its weight as the weight of the displaced liquid.

This principle illustrated for the example of a cuboid, is valid for any body with arbitrary shape as can be seen from the following consideration:

Due to the hydrostatic pressure $p = \varrho_{fl} \cdot g \cdot (H - z)$ at the height z in a liquid with total height H the force on a volume element dV is

$$\begin{aligned} \boldsymbol{F} &= -\mathbf{grad}\, p \cdot dV = -(\partial p/\partial z)\hat{\boldsymbol{e}}_z dV = \varrho_L \cdot g \cdot dV \cdot \hat{\boldsymbol{e}}_z \\ &= -\varrho_L \cdot \boldsymbol{g} \cdot dV \, . \end{aligned}$$

The buoyancy force on the whole body immersed in the liquid is then

$$\boldsymbol{F}_B = -\boldsymbol{g} \int \varrho_L \cdot dV = -\boldsymbol{G}_L \, . \qquad (6.33)$$

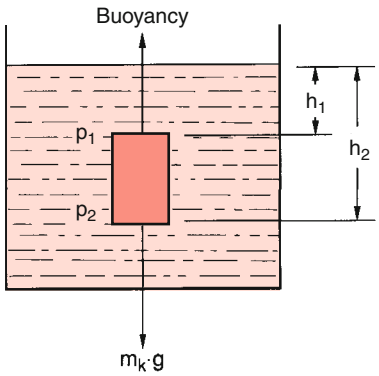

Figure 6.28 Axiom of Archimedes and buoyancy

If the density ϱ_b of a body is smaller than the density ϱ_L of the liquid, the buoyancy force becomes larger than the weight G_b of the body and the body floats on the surface of the liquid. Only part of the body immerses while the other part is above the liquid surface. Equilibrium is reached if the buoyancy (it is the weight G_L of the displaced liquid) just cancels the weight G_b of the total body.

Example

The density of ice is $\varrho_i = 0.95\,\mathrm{kg/dm^3}$, the density of salty sea-water at 0 °C is $\varrho_L = 1.05\,\mathrm{kg/dm^3}$. Therefore, about 10% of the volume of an iceberg stick out of the ocean surface, 90% are under water. ◀

Remark. Of course, the buoyancy is also present in gases. However, because of the much smaller density of gases the buoyancy force is correspondingly smaller. A body in a gas atmosphere loses (seemingly) as much of its weight as the weight of the displaced gas. This is the basis for balloon flights (see Sect. 7.2 and Fig. 7.6.

For the stability of a floating ship it is important that in case of heeling induced by waves there is always a restoring torque which brings the ship back into its vertical position. This stability criterion can be quantitatively formulated in the following way:

We consider the torque generated by the gravity force G_g and the buoyancy F_B for a ship in an oblique position (Fig. 6.29). The two forces form a couple of forces (Sect. 5.4) which cause a torque about the center of mass S_K. The point of origin for the gravity force G_g is the center of mass S_K of the ship, while the point of origin for the buoyancy $F_B = -G_g$ is the center of mass S_B of the displaced water. The symmetry plane of the ship, indicated in Fig. 6.29b by the dashed line, intersects the vertical direction of the buoyancy in the point M, called the *meta-center*. The vector $\boldsymbol{r}$ gives the distance between M and S_K. As long as M lies above S_K the resulting torque

$$\boldsymbol{D} = (\boldsymbol{r} \times \boldsymbol{G}_K) = -(\boldsymbol{r} \times \boldsymbol{F}_B) \,,$$

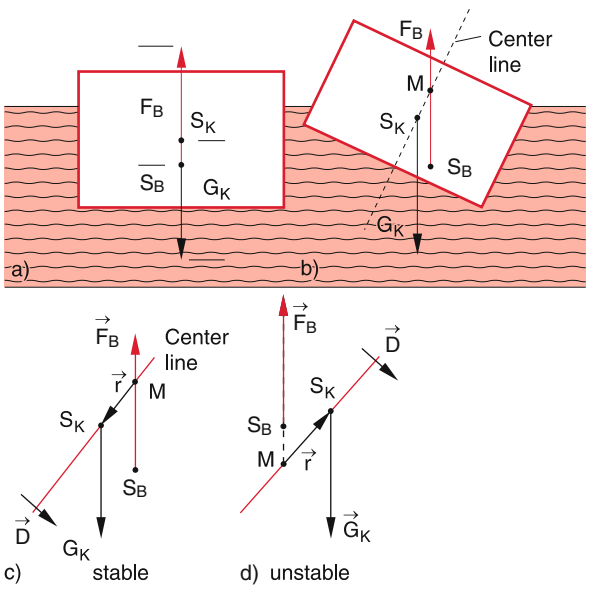

Figure 6.29 Stability of a floating body. **a** equilibrium position, **b** tilting below the critical angle, **c** vector diagram of stable and unstable heeling

which has in Fig. 6.29c the counter-clockwise direction, brings the ship back into the vertical stable position. If the slope becomes so large that M comes below S_K (Fig. 6.29d) the resulting torque acts into the clockwise direction and it brings the ship into a larger slope. It overturns and sinks. It is therefore advantageous for the stability to have the center of mass S_K as low as possible. This can be achieved by putting heavy masses at the bottom of the ship. In case of container ships, the cargo is loaded on top of the ship which decreases the stability. These ships have therefore a double mantel at the bottom where the interspace is filled with water, in order to bring the center of mass down.

6.4 Phenomena at Liquid Surfaces

We will now upgrade our simple model of the ideal liquid in order to introduce effects which occur at surfaces of real liquids and which are not present in ideal liquids. While inside a liquid the resulting time-averaged force on an arbitrary molecule, exerted by all other molecules, is zero, (this allows the free relocatability of each molecule), this is no longer true for molecules at the surface of liquids (Fig. 6.30) which are only attracted by molecules in a half sphere inside the liquid. Therefore a residual force $\boldsymbol{F}_R$ remains, which attracts the molecules towards the interior of the liquid.

6.4.1 Surface Tension

If a molecule is brought from the inside of a liquid to the surface, energy has to be supplied to move the molecule against the residual force F_R. A molecule at the surface has therefore a higher

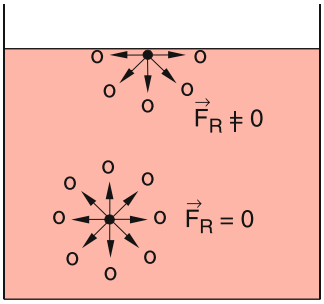

Figure 6.30 Resulting force on a molecule by all other surrounding molecules inside a liquid and at the surface of a liquid

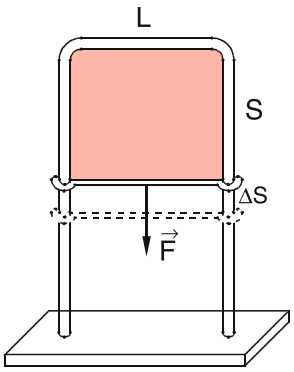

Figure 6.31 Determination of surface tension by measuring the force on a sliding straight wire, that extends a liquid skin

energy than a molecule inside the liquid. In order to enlarge the surface by an amount ΔA molecules have to be transferred to the surface which needs the energy ΔW. The ratio

$$\varepsilon = \frac{\Delta W}{\Delta A}\ ; \quad [\varepsilon] = \frac{\mathrm{J}}{\mathrm{m}^2} \tag{6.34}$$

is the *specific surface energy*. The value of ε depends on the binding forces between the molecules of the liquid. It can be measured with the equipment shown in Fig. 6.31. Between the two sides of a U-shaped frame a horizontal wire with length L can be shifted vertically. When the system is dipped into a liquid, a liquid lamella is formed with the surface area (on both sides) $A = 2L \cdot s$. For moving the horizontal wire by Δs, the force F is necessary. One has to supply the energy

$$\Delta W = \boldsymbol{F} \cdot \Delta s = \varepsilon \cdot \Delta A = \varepsilon \cdot 2 \cdot L \cdot \Delta s\ . \tag{6.35}$$

The restoring force $\boldsymbol{F}$, which is directed tangential to the surface of the lamella, produces a tensile strain $\sigma = F/2L$ per length unit which is called *surface tension*. According to (6.35) is

$$\sigma = \varepsilon\ .$$

Surface tension σ and specific surface energy ε are identical.

The surface tension can be impressively demonstrated by the apparatus shown in Fig. 6.32. A metal strip bent into a circle hangs

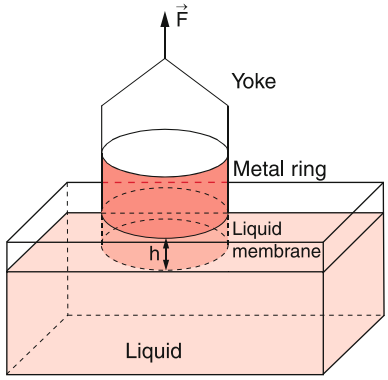

Figure 6.32 Measurement of surface tension by liftig an immersed metal ring

on a spring balance. It is immersed into a glass container filled with a liquid. When the container is lowered or the metal ring is uplifted, the lower rim of the ring emerges more and more out of the liquid, carrying a cylindrical liquid lamella. With soapy water more than 10 cm heights of the lamella can be reached. The spring balance measures the force

$$F = 4\pi \cdot r \cdot \sigma\ ,$$

because the lamella has two surfaces, inside and outside of the cylindrical membrane. The work necessary to lift the lamella up to the height h is

$$W = 4\pi \cdot r \cdot \sigma \cdot h\ .$$

Example

Surface tension and pressure in a soap bubble (Fig. 6.33). Because of its surface tension, the bubble tries to reduce its surface. This increases the pressure inside the bubble. Equilibrium is reached, if the work against the increasing pressure during the decrease Δr of the bubble radius is equal to the work gained by the reduction ΔA of the surface area A

$$\varepsilon \cdot 2 \cdot 4\pi(r^2 - (r - \Delta r)^2) = 4\pi \cdot r^2 \cdot \Delta p\ .$$

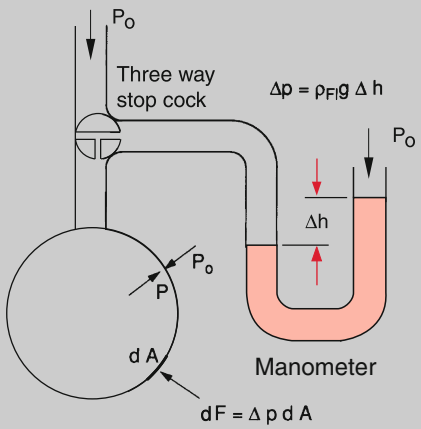

Figure 6.33 Measurement of overpressure Δp in a soap bubble, caused by surface tension

Neglecting the term with $(\Delta r)^2$ gives the excess pressure

$$\Delta p = 4\varepsilon/r\,, \tag{6.36}$$

which shows that Δp decreases with increasing radius r. This can be demonstrated by the equipment in Fig. 6.34. The lower ends of the tubes 1 and 2 are immersed into soapy water and then lifted again. With open valves 1 and 2 but closed valve 3, two bubbles with different sizes can be produced by blowing air into the corresponding filling tubes. Now valves 1 and 2 are closed and valve 3 is opened. The smaller bubble starts to shrink and the larger one inflates. This continues until the smaller bubble completely disappears. It's like in daily life. The powerful people (larger ones) increase their power at the cost of the little guys.

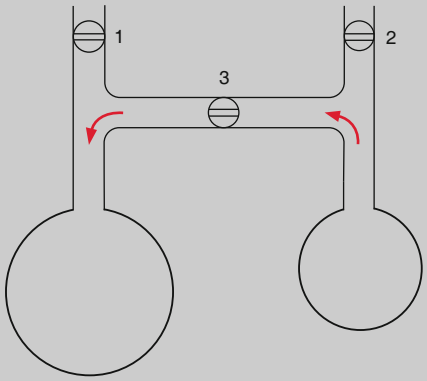

Figure 6.34 Demonstration of overpressure $\Delta p(r)$ which increases with decreasing radius r of a soap bubble

For liquids with positive surface energy each liquid with a given volume tries to minimize its surface area.

This can be demonstrated by adding drop wise mercury through a pipette into a bowl filled with diluted sulfur acid. At first many small mercury droplets are formed which, however, soon merge into a single larger drop. ◀

6.4.2 Interfaces and Adhesion Tension

Up to now, we have only discussed surfaces of liquids as boundaries between liquid and gaseous phases. Often interfaces between different liquids or between liquid and solid bodies can occur. Analogue to the surface tension we define the boundary tension σ_{ik} (identical with the specific interface energy ε_{ik}) as the energy that has to be spend (or is gained) when the interface between the phases i and k is increased by 1 m^2.

The sign of ε_{ik} can be obtained by the following considerations:

- For stable interfaces between liquid and gas ε_{ik} has to be positive. Otherwise the liquid phase would be transferred into the gas phase because energy would be gained, i.e. the liquid would vaporize.
- Also for stable interfaces between two different liquids ε_{ik} must be positive. Otherwise the two liquids would intermix and the interface would disappear.
- For the interface between liquid and solid phases the sign of ε_{ik} depends on the materials of the two phases. If the molecules M_L in the liquid are attracted more strongly by the molecules M_s in the solid, than by neighboring molecules in the liquid, is $\varepsilon_{ik} < 0$. If the attracting forces between molecules M_L are stronger than between M_L and M_s is $\varepsilon_{ik} > 0$.
- Also between a solid surface and a gas an interface energy can occur, because the gas molecules can be attracted by the solid surface (adhesion) or they can be repelled, depending on the gas and the solid material.

We will illustrate these points by some examples: In Fig. 6.35 is the surface of a liquid 2 against the gas phase 3 close to a vertical solid wall 1 depicted. Here the surface tensions $\sigma_{1,2}$; $\sigma_{1,3}$ and $\sigma_{2,3}$ tangential to the corresponding surfaces have to be considered. We regard a line element dl perpendicular to the plane of the drawing through the point A, where all three phases are in contact with each other. The force parallel to the solid surface is $F_{\parallel s} = (\sigma_{1,2} - \sigma_{1,3})\mathrm{d}l$ and $F_{\parallel l} = \sigma_{2,3}\mathrm{d}l$ is parallel to the liquid surface. The resulting force causes a change of the liquid

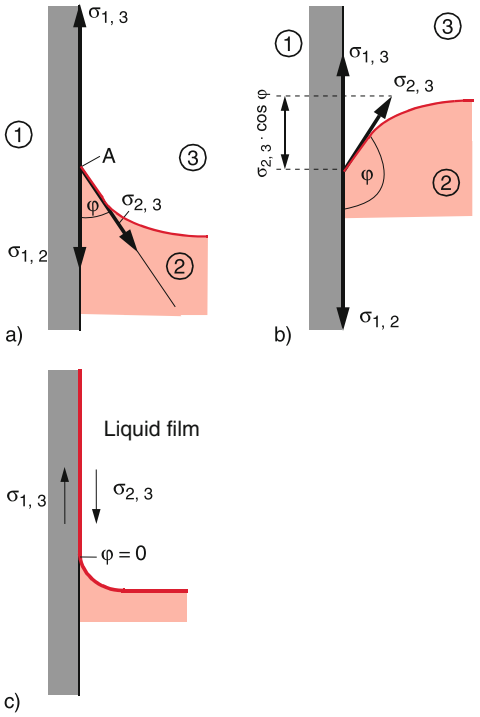

Figure 6.35 Formation of a contact angle of a liquid surface with a vertical solid wall. **a** Concave liquid surface for water-glass ($\sigma_{1,3} > \sigma_{1,2}$); **b** convex surface of Hg-glass ($\sigma_{1,3} < \sigma_{1,2}$); **c** complete wetting for $\sigma_{1,3} - \sigma_{1,2} > \sigma_{2,3}$

surface, which would be a horizontal plane under the action of gravity without surface tension.

If we neglect the small change of the gravitational force due to the change of the surface, which is very small compared to the forces caused by surface tension, we have the equilibrium condition that in the point A the vector sum of all forces must be zero. For the vertical component parallel to the solid wall this implies:

$$\sigma_{1,2} + \sigma_{2,3} \cos\varphi - \sigma_{1,3} = 0 \,. \tag{6.37}$$

The horizontal component $\sigma_{2,3} \cdot \sin\varphi$ causes an imperceptibly small deformation of the solid wall. This induces a restoring deformation force which is opposite to the force $\sigma_{2,3}$ and has the same magnitude and therefore compensates it. The wetting angle φ can be obtained from the condition

$$\cos\varphi = \frac{\sigma_{1,3} - \sigma_{1,2}}{\sigma_{2,3}} \,. \tag{6.37a}$$

It has a definite value only for $|\sigma_{1,3} - \sigma_{1,2}| \leq \sigma_{2,3}$. We distinguish the following cases:

- $\sigma_{1,3} > \sigma_{1,2} \rightarrow \cos\varphi > 0 \rightarrow \varphi < 90°$.
  The liquid forms close to the solid wall a concave surface, which forms an acute angle φ with the wall (Fig. 6.35a). It is energetically favorable to increase the interface liquid-solid at the cost of the interface solid–gas.
  Example: Interfaces water–glas–air.
- $\sigma_{1,3} < \sigma_{1,2} \rightarrow \cos\varphi < 0 \rightarrow \varphi > 90°$.
  The liquid forms close to the solid wall a convex surface (Fig. 6.35b).
  Example: interfaces mercury–glas–air.
- For $|\sigma_{1,3} - \sigma_{1,2}| > \sigma_{2,3}$ Eq. 6.37 cannot been fulfilled for any angle φ. In this case a force component parallel to the solid surface is uncompensated. It pulls the liquid along the solid surface until the whole surface is covered by a liquid film (Fig. 6.35c). The interface solid–gas disappears completely.

If external forces are present, such as gravitational or inertial forces in accelerated systems, the vector sum of all forces is in general not zero. However, the liquid surface reacts always in such a way, that the resultant force is perpendicular to the liquid surface, i.e. its tangential component is always zero. This is illustrated in Fig. 6.36 for the cases of a concave and a convex curvature of the liquid surface close to the solid wall where besides the gravitational force also the attractive force F_4 between liquid and solid surfaces is taken into account.

For a liquid in a container the total force is compensated by the restoring elastic force of the container wall.

For two non-mixable liquids 1 and 2 (for example a fat drop on water) the angles φ_1 and φ_2 in Fig. 6.37 adjust in such a way that the equilibrium condition

$$\sigma_{1,3} = \sigma_{2,3} \cos\varphi_2 + \sigma_{1,2} \cos\varphi_1 \tag{6.38}$$

is fulfilled. This shows that a droplet of the liquid 2 can be only formed, if $\sigma_{1,3} < \sigma_{2,3} + \sigma_{1,2}$. Otherwise the droplet would be spread out by the surface tension $\sigma_{1,3}$ until it forms a thin film, which covers the surface of liquid 1.

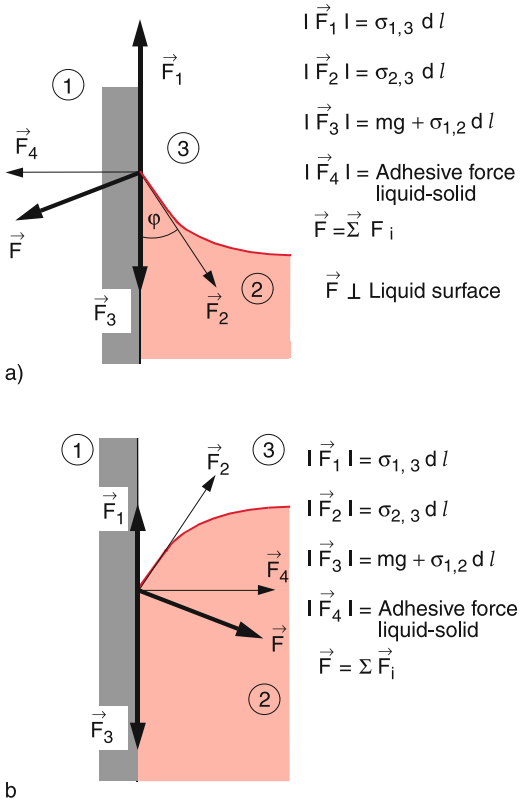

Figure 6.36 The vector sum of all forces acting onto a liquid sureface must be always vertical to the surface, for non-wetting liquids. **a** Concave, **b** convex curved surface

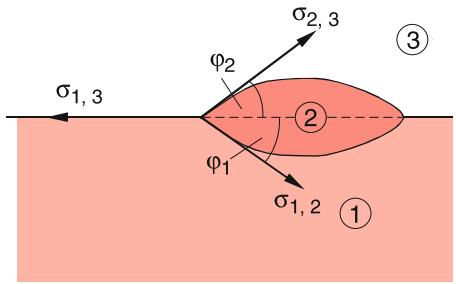

Figure 6.37 Formation of a liquid drop on the surface of another liquid

Example

For the interfaces water–oil–air the numerical values of the surface tensions are:

$$\sigma_{1,3}(\text{water-air}) = 72.5 \cdot 10^{-3}\,\text{J/m}^2$$
$$\sigma_{1,2}(\text{water-oil}) = 46 \cdot 10^{-3}\,\text{J/m}^2$$
$$\sigma_{2,3}(\text{oil-air}) = 32 \cdot 10^{-3}\,\text{J/m}^2 \,.$$

This shows that $\sigma_{1,3} > \sigma_{2,3} + \sigma_{1,2}$. Therefore, oil cannot form droplets on a water surface. ◀

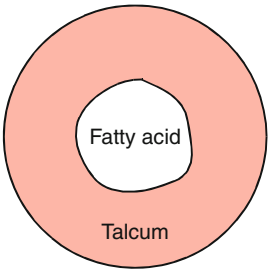

Figure 6.38 Formation of a mono-molecular layer of a fatty acid on a liquid surface covered with a talcum powder layer

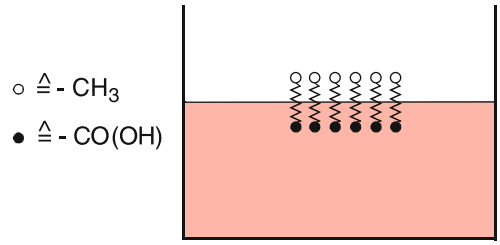

Figure 6.39 Fatty acid molecules forming a mono-molecular layer on a water surface are oriented due to the attractive for one end of the interaction with the water molecules and a repulsive interaction for the other end

If an oil drop is brought onto a water surface, it will spread out to form a mono-molecular layer of oil which covers the whole water surface if sufficient oil is contained in the drop. Otherwise, the oil film forms a cohesive insula of this mono-molecular film. This can be demonstrated by the following experiment (Fig. 6.38): Onto a water surface, powdered with talc, a droplet of fatty acid is supplied through a pipette. The droplet immediately spreads out and displaces the talc layer. The fatty acid molecules are oriented in such a way, that the attractive force with the water molecules becomes maximum (Fig. 6.39). The atomic groups COOH, which are directed against the water surface, are called *hydrophilic* while the groups on the opposite side of the molecule, which are repelled by the water molecules, are called *hydrophobic*. The interaction with the water molecules causes a displacement of the charges in the fatty acid molecules while the water molecules, which are electric dipoles, are orientated in such a way, that their positive pole is directed toward the negative pole of the induced dipole molecules of the fatty acid (see Vol. 2, Chap. 2).

6.4.3 Capillarity

When a capillary tube is dipped into a wetting liquid ($\sigma_{1,3} > \sigma_{1,2}$), the wetting liquid rises in the capillary tube up to the height h above the liquid surface (Fig. 6.40). This observation can be explained as follows: If a liquid column in the capillary with radius r is lifted up to the height h ($h \gg r$) the potential energy is increased by

$$dE_p = m \cdot g \cdot dh = \pi \cdot r^2 g \cdot \varrho \cdot h \cdot dh \; . \tag{6.39a}$$

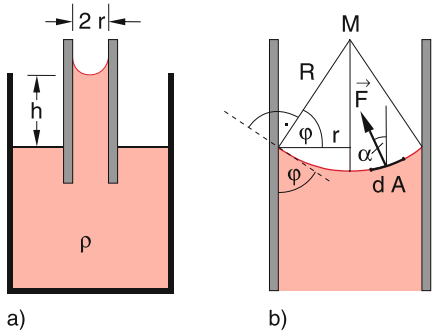

Figure 6.40 **a** Capillary rise of a wetting liquid, **b** derivation of the rise height

On the other hand, the surface energy changes by (see Fig. 6.36)

$$\begin{aligned} dE_{surface} &= -2\pi r \cdot dh(\sigma_{13} - \sigma_{12}) \\ &= 2\pi r \cdot dh \cdot \sigma_{23} \cdot \cos\varphi \; , \end{aligned} \tag{6.39b}$$

where Eq. 6.37a has been used. At equilibrium is $dE_p + dE_{surface} = 0$. This gives the resulting height

$$\begin{aligned} h &= 2\sigma_{23} \cdot \cos\varphi/(r \cdot g \cdot \varrho) \\ &= 2\sigma \cdot \cos\varphi/(r \cdot g \cdot \varrho) \; . \end{aligned} \tag{6.40}$$

The wetting angle φ is determined by Eq. 6.37). The surface tension $\sigma_{2,3} = \sigma$ is the surface tension of the liquid against air, introduced in Sect. 6.4.1.

For completely wetting liquids ($\sigma_{1,3} > \sigma_{1,2} + \sigma_{2,3}$) is $\varphi = 0$. The complete inner surface of the capillary tube is covered by a thin liquid film and the capillary rise becomes according to (6.40)

$$h = \frac{2\sigma}{rg\varrho} \; . \tag{6.40a}$$

For non-wetting liquids ($\sigma_{1,3} < \sigma_{1,2}$) the liquid surface inside the capillary is convex. This convex curvature causes a force, which is directed downwards and leads to a capillary depression (Fig. 6.41). The depression height $-h$ is again given by (6.40), where now $\cos\varphi = (\sigma_{1,3} - \sigma_{1,2})/\sigma_{2,3} < 0$.

The capillary rise offers an experimental method for the measurement of absolute values of surface tensions. Instead of

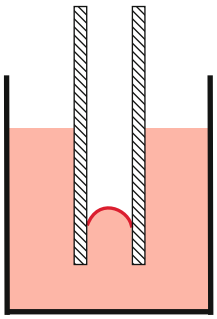

Figure 6.41 Capillary depression

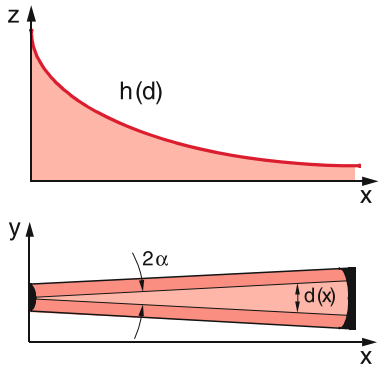

Figure 6.42 Demonstration of capillary rise $h(d) \propto 1/d$ of a liquid confined between two wedged plane walls with the wegde angle 2α

capillary tubes one can also use two parallel plates with the distance d. A liquid between these plates has the capillary rise

$$h = \frac{2\sigma}{\varrho g} \cdot \frac{1}{d} \,. \tag{6.41}$$

The dependence $h(d)$ can be demonstrated by two nearly parallel plates, which are slightly inclined against each other by a small angle α (Fig. 6.42). Since the distance $d(x) = 2x \cdot \tan\alpha$ increases linearly with x the height $h(x) \propto 1/x$ is a hyperbola.

6.4.4 Summary of Section 6.4

The many different phenomena at the boundaries of liquids can be all quantitatively explained by the magnitude of the surface tensions or surface energies. We can make the following statements:

- At each point of a stable liquid surface the total force is always perpendicular to the surface, its tangential component is zero.
- The boundary of a liquid with a given volume always approaches that shape that has the minimum surface area.
- A bent convex liquid surface with radius of curvature r produces an inward pressure, that is proportional to $1/r$ and to the surface tension.

6.5 Friction Between Solid Bodies

If two moving extended bodies touch each other, additional forces occur which depend on the properties of the two surfaces. Examples are a metal block sliding on a plane base, or a wheel rotating around an axis. These forces are due to the interaction between the atoms or molecules in the outer layers of the two bodies. This interaction is reinforced by surface irregularities and deformations, caused by the contact between the two bodies. These forces are called *friction forces*. For point masses they can be completely neglected because their surface area is zero. In daily life and for technical problems they play a very important role. Without friction we would not be able to walk nor cars could run. Also most technical processes of machine work on material, such as drilling, milling or cutting would not be possible without friction. On the other hand, often friction needs to be minimized in order to avoid energy dissipation.

We will therefore discuss the basic principles of friction phenomena in more detail.

6.5.1 Static Friction

A body with a plane base (for example a cuboid) rests on a horizontal plane table. In order to move it across the table we must apply a force in the horizontal direction, which can be measured with a spring balance (Fig. 6.43a). The experiment shows that in spite of the applied force the body with mass m does not move until the force exceeds a definite value F_s. When the body is turned over (Fig. 6.43b) so that now another surface with a different area touches the table, this critical force F_s does not change in spite of the different surface area in contact with the table. However, if the body is pressed by an additional force against the table, the critical pulling force F_s increases. The experiments show, that F_s is proportional to the total vertical force F_N exerted by the body on the table and on the roughness of the two surfaces in contact.

The amount of this static friction force is

$$F_s = \mu_s \cdot F_N \,. \tag{6.42}$$

The static friction coefficient μ_s depends on the materials of the bodies in contact and on the texture of the two surfaces.

The static friction can be explained in a simple model (Fig. 6.44) by the roughness of the two surfaces in contact. Even a polished plane surface is not an ideal plane but shows microscopic deviations from the ideal plane, which may be caused by lattice defects, shifts of atomic planes etc. The envelope of this microroughness gives the macroscopic deviations caused by imperfect polishing or grinding. A measure for these deviations is the mean quadratic deviation $\langle z^2(x,y)\rangle$ from the ideal plane $z = 0$. Since one measures generally not single points but surface elements $dx \cdot dy$, the function $z(x,y)$ is averaged over the surface

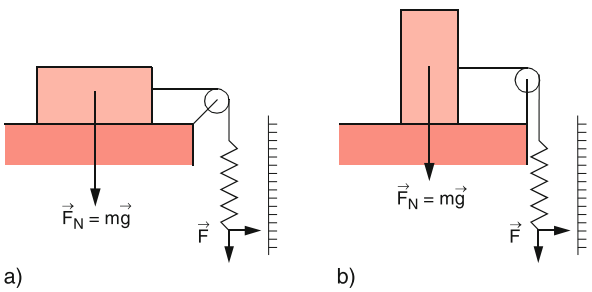

Figure 6.43 Measurement of static friction with a spring balance

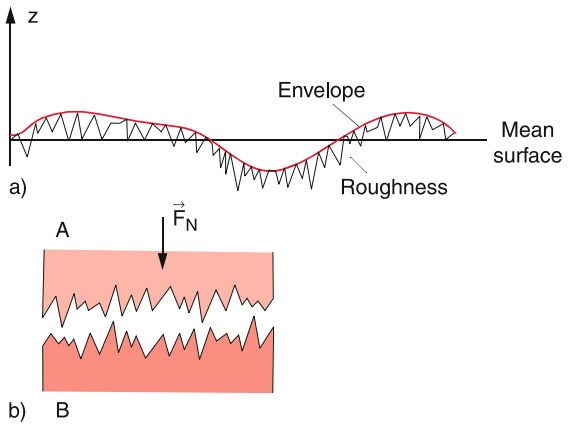

Figure 6.44 Schematic model of the surface roughness as the cause of friction. **a** micro roughness (exagerated) and macroscopic coarseness; **b** static friction caused by interlocking of two rough surfaces

elements $dx \cdot dy$ and this average depends on the spatial resolution of the analyzing instrument i.e. on the size of the resolved elements $dx \cdot dy$. With modern surface analysis, using tunnel-microscopes (see Vol. 3) even the roughness on an atomic scale can be spatially resolved.

The two surfaces in contact interlock each other due to the force that presses them together (Fig. 6.44b) and the force F_s is necessary to release this interlocking. This can be achieved by breaking away the "hills" of the rough surface, or by lifting the body over these hills.

A possible way to determine experimentally the coefficient of static friction uses the inclined plane with a variable inclination angle α in Fig. 6.45. The angle α is continuously increased until the body B with mass m starts to slide down for $\alpha = \alpha_{max}$.

The weight force $\boldsymbol{G} = m \cdot \boldsymbol{g}$ can be decomposed into two components:

1. A component $F_{\parallel} = m \cdot g \cdot \sin\alpha$ parallel to the inclined plane

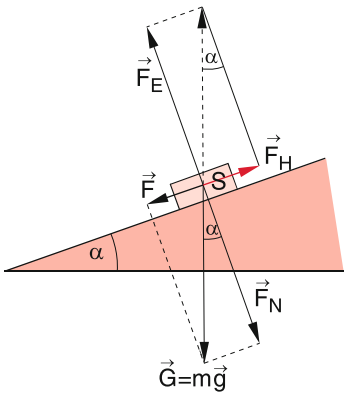

Figure 6.45 Measurement of coefficient of static friction with the inclined plane

2. A component $F_{\perp} = m \cdot g \cdot \cos\alpha$ perpendicular to the inclined plane, which is compensated by the opposite restoring force of the elastic deformation of the plane.

The body starts to slide downwards as soon as $F_{\parallel}$ becomes larger than the static friction force $F_s = \mu_s \cdot F_{\perp} = \mu_s \cdot m \cdot g \cdot \cos\alpha$. This gives the condition for the coefficient μ_s

$$\mu_s = \frac{F_{\parallel}(\alpha_{max})}{F_{\perp}(\alpha_{max})} = \tan\alpha_{max} \ . \tag{6.43}$$

If α is increased beyond α_{max} the body performs an accelerated sliding motion. This indicates that the sliding friction force is smaller than the static friction force.

6.5.2 Sliding Friction

When the body in Fig. 6.43 is moved by a force $|\boldsymbol{F}| > |\boldsymbol{F}_s|$ the sliding motion is accelerated. In order to reach a uniform motion of a sliding body with constant velocity, where the total force is zero, one needs only the smaller force $|\boldsymbol{F}_{sl}| < |\boldsymbol{F}_s|$. Analogue to the static friction force, the sliding friction force F_{sl} is proportional to the force F_N normal to the surface of the table on which it slides.

$$\boldsymbol{F}_{sl} = \mu_{sl} \cdot \boldsymbol{F}_N \ . \tag{6.44}$$

The coefficient of sliding friction μ_{sl} depends again on the material of body and basis, but also on the relative velocity. It is, however, always smaller than the coefficient of static friction. This can be explained by the simplified model of the two surfaces in contact, shown schematically in Fig. 6.44, where the roughness of the surfaces has been exaggerated. If the two bodies are at rest the peaks and the valleys of the micro-mountains interlock. This allows a minimum distance between the two attracting surfaces resulting in a minimum energy. At the sliding motion the two surfaces move above the peaks and the mean distance between the surfaces is larger. During the sliding motion, parts of the peaks are ablated. This results in an attrition of the surfaces.

The sliding motion dissipates energy, even for a horizontal motion. If the body is moved by the distance Δx, the necessary work is $W = F_{sl} \cdot \Delta x$, which is converted into heat.

Experiments show that the sling friction force increases with the relative velocity. The reason is that with increasing velocity more material of the two surfaces is ablated. The power $P = dW/dt$, necessary to maintain the velocity v of a sliding motion, increases with v^n where $n > 1$.

Note: The friction between a moving body and the surrounding air has different reasons. If the body moves through air at rest, a thin layer of air close to the surface of the body sticks at the surface and is therefore accelerated by the moving body. This requires the energy $1/2 m_L \cdot v^2$ where m_L is the mass of the air layer that also increases with the velocity v.

6.5.3 Rolling Friction

When a round body rolls over a surface, also friction forces F_R occur which are caused by the interaction between the atoms of the bodies at the line of contact. Furthermore, the base is deformed by the weight of the round body (Fig. 6.46), which leads to deformation forces. For the rolling of a round body with constant angular velocity, a torque around the contact line is necessary that just compensates the opposite torque of the rolling friction. Around the depression of the base at the line of contact, bulges are formed, which have to be overcome when the body rolls.

The experiments tell us that the torque, necessary for keeping a constant angular velocity, is proportional to the force F_N normal to the surface of the base

$$D_R = \mu_R \cdot F_N \,, \tag{6.45}$$

where the coefficient μ_R of rolling friction has the dimension of a length in contrast to the dimensionless coefficients μ_s and μ_{sl}.

Similar to the measurement of μ_s the coefficient μ_R can be measured with an inclined plane (Fig. 6.47). A circular cylinder with mass m and radius r does not roll down the inclined plane, if the inclination angle α is smaller than a critical angle α_R, which is, however, smaller than the angle α_{max} measured for the static friction in Fig. 6.45.

For this critical angle α_R is the counter-clockwise torque $D_G = m \cdot g \cdot r \cdot \sin\alpha_R$ around the contact line just equal to the clockwise torque $D_R = \mu_R \cdot F_N = \mu_R \cdot m \cdot g \cdot \cos\alpha_R$. This yields

$$\mu_R = r \cdot \tan\alpha_R \,. \tag{6.46}$$

The rolling friction is proportional to the radius of the round body. The rolling friction is much smaller than the sliding friction, because the surface irregularities, shown in Fig. 6.44, are partly overrun. Therefore, the invention of the wheel was a great progress for humankind. The comparison of the frictional forces for sliding and rolling gives with (6.44) and (6.45) the ratio

$$\frac{F_s}{F_R} = \frac{F_s}{F_R/r} = r \cdot \frac{\mu_s}{\mu_R} \,. \tag{6.47}$$

The much smaller rolling friction is utilized by ball bearings, which reduce the friction of rotating axes compared to the sliding friction without these ball bearings. In Fig. 6.48, some technical realizations of different ball bearings and axial bearings are shown. In Tab. 6.3, the friction coefficients for some materials are listed.

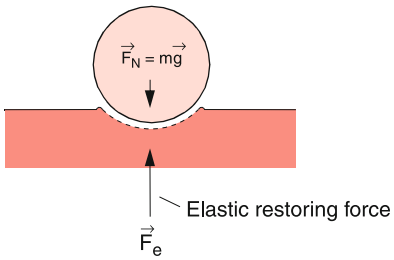

Figure 6.46 Deformation of a surface around the contact line

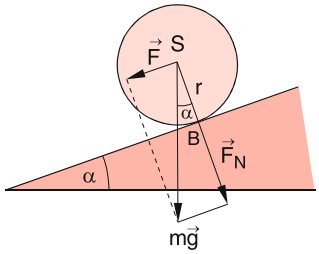

Figure 6.47 Measurement of rolling friction with the inclined plane

Remark. For skating or tobogganing the snow melts under the runners because of heat conduction from the warmer skates and due to the heat produced by friction. The water film under the vats reduces the friction considerably. Often one finds the explanation that the pressure exerted by the weight of the skater is the main reason for melting. This effect plays, however, only a minor part, as can be calculated from the known decrease of the melting point with increasing pressure. (see Sect. 10.4.2.4). The much smaller sliding friction between solid surface and liquids is also utilized by applying lubricants between the two surfaces, for instance between a rotating axis and its fixed support or between the moving pistons of a car engine and the cylinders. The oil film reduces the friction by about two orders of magnitude.

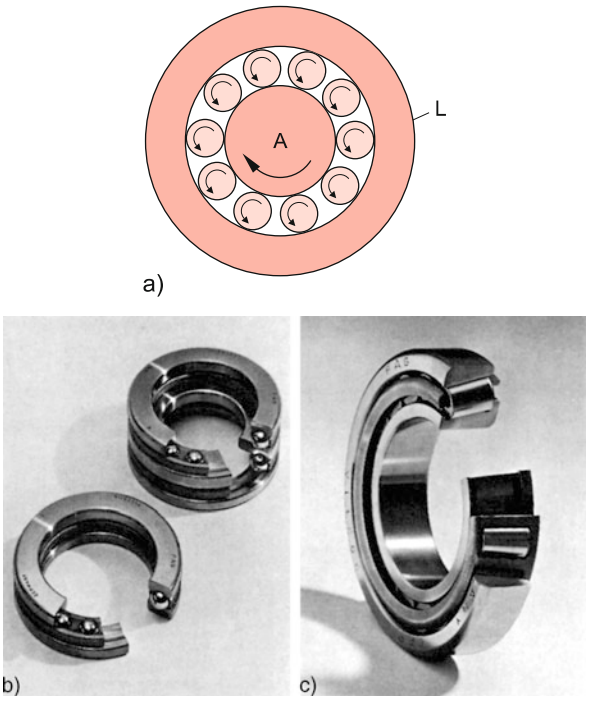

Figure 6.48 Ball bearings. **a** scheme of a radial grooves bearing; **b** realization; **c** axial groove bearing

Table 6.3 Coefficients of static, sliding and rolling friction of some materials in contact with each other. The values strongly depend of the characteristics of the surfaces. They therefore differ for different authors

Interacting materials	μ_H	μ_G	μ_R/r
Steel–Steel	0.5–0.8	0.4	0.05
Steel with oil film	0.08	0.06	0.03–0.1
Al–Al	1.1	0.8–1.0	
Steel–Wood	0.5	0.2–0.5	
Wood–Wood	0.6	0.3	0.5
Diamond–Diamond	0.1	0.08	
Glass–Glass	0.9–1.0	0.4	
Rubber-tar seal			
– dry	1.2	1.05	
– wet without waterfilm	0.6	0.4	

6.5.4 Significance of Friction for Technology

Friction plays an outstanding role for many technical problems. In some cases it should be as large as possible (for example for clutches in cars or other machinery). The rolling friction for car tires should be as small as possible, but the static friction and the sliding friction should be as large as possible.

For many sliding or rotating parts of machinery, friction is damaging. It causes increased energy consumption and a destruction of the sliding surfaces (attrition). For such cases, it is therefore necessary to minimize friction. This can be achieved either by reducing the sliding friction by liquid films or air buffers or by using ball bearings. Because of its importance, meanwhile a whole branch of science called *tribology* works on problems of friction [6.4].

Example

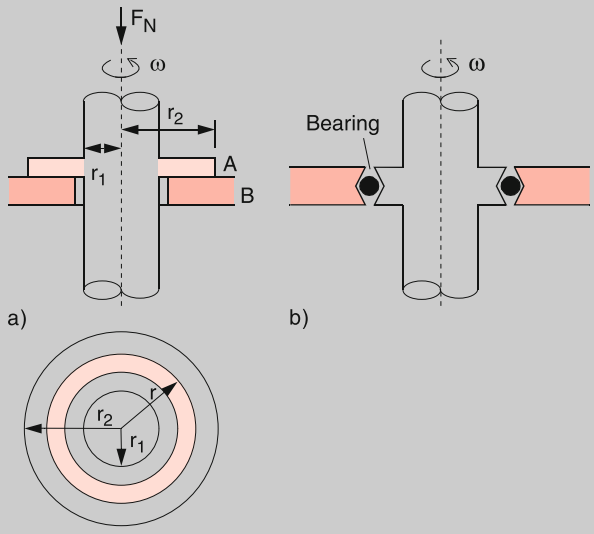

Figure 6.49 Rotating axis **a** without ball bearing, **b** with ball bearing

In Fig. 6.49a is an axis shown that rotates with the angular velocity ω. A circular ring with area $A = \pi(r_2^2 - r_1^2)$ is welded to the axis and exerts a force F_N and a pressure $p = F_N/A$ onto the support base. The sliding friction causes a torque D on the rotating axis, which has to be compensated by an opposite torque supplied by an external force.

On the red annulus in the lower part of Fig. 6.49a acts the force $dF_N = 2\pi \cdot r \cdot dr \cdot p$, which causes the torque $dD = r \cdot dF_s = \mu_s \cdot p \cdot 2\pi \cdot r^2 \cdot dr$. Integrating over all annuli gives the total torque

$$D = \int_{r_1}^{r_2} dD = \frac{2\pi}{3} \mu_{sl} \cdot p \cdot \left(r_2^3 - r_1^3\right) . \qquad (6.48)$$

The friction consumes the power $P = D \cdot \omega$, which is converted into heat. This dissipated power is proportional to the coefficient μ_s of sliding friction, to the contact pressure p and the angular velocity ω. If the annulus with area A is supported by ball bearings (Fig. 6.49b), the torque caused by friction decreases by some orders of magnitude. ◀

Another solution uses the mounting in Fig. 6.49a but now with a liquid film between the contacting surfaces. Often air is blown with high pressure between the two surfaces and an air buffer supports the rotating annulus.. This allows one to realize an extremely low friction. Examples are very fast rotating turbomolecular vacuum pumps (see Sect. 9.2.1.3), where the rotating blades are supported by the air blow.

6.6 The Earth as Deformable Body

At the end of this chapter, we will apply the results of the foregoing sections to the interesting example of our earth, which can be deformed by several forces acting on it. In addition friction plays an important role for phenomena such as the tides or the differential rotation of the inner parts of the earth. Since the earth is composed of solid material as well as of liquid phases, it gives a good example of a realistic and more complicated deformable body.

Our earth is not a rigid homogeneous sphere. It shows an inhomogeneous radial density profile $r(r)$ (Fig. 6.50), which is determined by the pressure profile $p(r)$, but also by the chemical composition, which changes with the radius r. Furthermore, the different solid and liquid phases in the interior of the earth contribute to the inhomogeneous profile. The central region with $r < 1000$ km is a solid kernel of heavy elements (iron, nickel), while for $r > 1000$ km hot liquid phases of metals are predominant, covered by a relatively thin solid crust, consisting of large plates, which float on the liquid material. The earth is therefore not a rigid body but can be deformed by centrifugal forces,

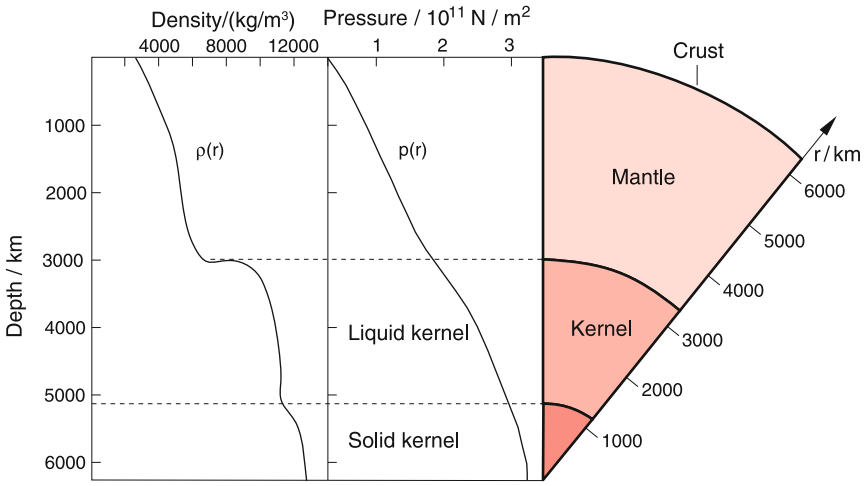

Figure 6.50 Radial density profile of the earth

caused by the earth rotation, and by gravitational, forces due to the attraction by the sun and the moon. These deformations are partly elastic (tides of the earth crust) or plastic (= inelastic). In the latter case, the deformed material does not come back to its original location after the force ends and a permanent change of the shape remains. The shift of the continental plates or the eruption of volcanos with the formation of new islands or mountains are examples of non-elastic deformations.

6.6.1 Ellipticity of the Rotating Earth

The rotation of the earth with the angular velocity $\omega = 2\pi/\text{day} = 7.3 \cdot 10^{-5}\,\text{s}^{-1}$ causes a centrifugal force on a mass element Δm with the distance a from the rotation axis

$$\boldsymbol{F}_{\text{cf}} = \Delta m \cdot a \cdot \omega^2 \cdot \hat{\boldsymbol{e}}_{\text{cf}} \qquad (6.49a)$$

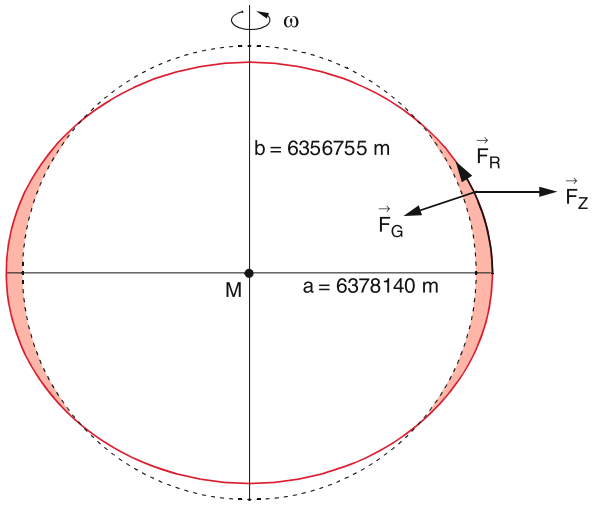

Figure 6.51 Deformation of the rotating earth due to centrifugal force

with the unit vector $\hat{\boldsymbol{e}}_{\text{cf}}$ perpendicular to $\boldsymbol{\omega}$. This force acts in addition to the gravitational force

$$F_{\text{G}} = -G \cdot \frac{\Delta m \cdot M(r)}{r^2}\hat{\boldsymbol{r}}\,, \qquad (6.49b)$$

where $M(r)$ is the mass of that part of the earth inside the radius r. Because of the plastic deformation the mass element Δm shifts until the total force $\boldsymbol{F}$ acting on it, is zero.

$$\boldsymbol{F} = \boldsymbol{F}_{\text{G}} + \boldsymbol{F}_{\text{cf}} + \boldsymbol{F}_{\text{R}}$$

is the sum of gravity force $\boldsymbol{F}_{\text{G}}$, centrifugal force $\boldsymbol{F}_{\text{cf}}$ and restoring force $\boldsymbol{F}_{\text{R}}$. For a homogeneous earth this would result in a rotational ellipsoid with the major diameter in the equatorial plane

$$2a = 12\,756.3\,\text{km}\,,$$

and with a minor diameter in the direction of the rotational axis of

$$2b = 12\,713.5\,\text{km}\,.$$

The ellipticity $\varepsilon = (a-b)/a$ of this rotational ellipsoid is $\varepsilon = 3.353 \cdot 10^{-3}$.

Because of the inhomogeneous mass distribution the shape of the rotating earth deviates slightly from this rotational ellipsoid but forms a nearly pear-shaped pattern called *geoid* (Fig. 2.56). The surface of this geoid is the zero-surface for all geodetic measurements. This means: all measurements of elevations z are related to this zero surface $z = 0$ [6.5].

6.6.2 Tidal Deformations

Induced by the additional forces of the gravitational attraction by the sun and the moon the earth surface deforms in a characteristic time-dependent way. This deformation is maximum for

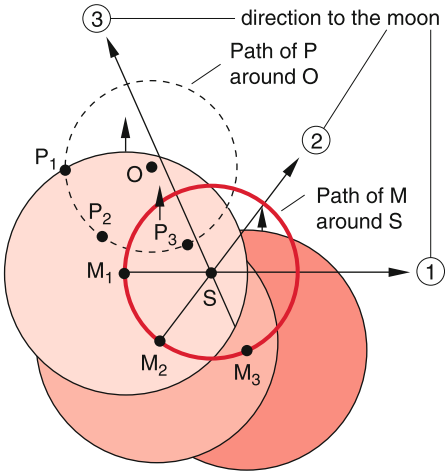

Figure 6.52 The rotation of earth and moon about their common center of mass S causes all points of the earth to rotate about the center S, that moves with the revolution of the moon. This is shown, without the daily rotation of the earth about its axis, for three different positions of the moon

the oceans (low tides and high tides) since for liquids the restoring elastic force is zero. However, it also appears with smaller elongation in the solid crust of the earth.

The deformation of the earth and the resulting tides have three causes:

a) The centrifugal distortion due to the motion of earth and moon about their common center of mass.
b) The gravitational force, effected by the masses of moon and sun.
c) The centrifugal distortion due to the rotation of the earth around its axis.

In order to understand this tidal deformation we discuss at first the simplified model of the deformation of the non-rotating earth and neglect the gravitational attraction by the sun and the revolution of the earth around the sun. We restrict the discussion therefore to the influence of the moon on the non-rotating earth. Under the mutual gravitational attraction

$$\boldsymbol{F}_{\mathrm{G}} = -G \cdot \frac{M_{\mathrm{E}} \cdot M_{\mathrm{Mo}}}{r_0^2} \hat{\boldsymbol{r}}_0 \,, \tag{6.50}$$

earth and moon move around their common center of mass S (also called bari-center) which lies still inside the earth (about 0.75 of the earth radius from the center). The distance between the centers of earth and moon is r_0. During a moon-period of 27.3 days the center M of the earth moves on a circle with radius $0.75R$ around the baricenter S, which always lies on the line M_{E}-M_{Mo}. All arbitrary points P_i in the earth move around S on circles with radii $P_i - S$. However, the center of mass S has no fixed position inside the earth but moves during one moon period inside the earth on a circle with radius $0.75R_{\mathrm{E}}$ around the center M of the earth, because the space-fixed center of mass S lies always on the line between earth-center and moon center.

The motion of the non-rotating earth as extended body, described in the coordinate system of the earth, is therefore **not** a

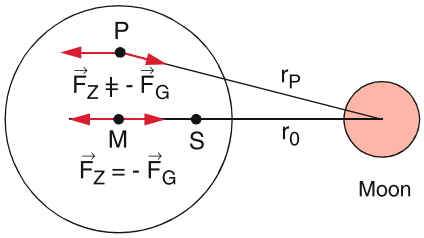

Figure 6.53 Only for the center M of the earth are gravitational attraction by the moon and centrifugal force of the earth–moon rotation about S equal but opposite and cancel each other

rotation about a fixed axis but rather a shift since the space-fixed point S. has not a fixed location inside the earth. The revolution of the moon and the earth about S with the angular velocity Ω causes therefore for all points of the non-rotating earth the same centrifugal force

$$F_{\mathrm{cf}} = m\Omega^2 \cdot R_{\mathrm{S}} = m\Omega^2 \cdot 0.75R \,. \tag{6.51}$$

On the other hand, the gravitational attraction between earth and moon is different for the different points of the earth because of their different distance from the moon center. For the earth center M it is

$$\boldsymbol{F}_{\mathrm{G}} = -G\frac{M_{\mathrm{E}} \cdot M_{\mathrm{Mo}}}{r^2}\hat{\boldsymbol{r}}_0 \tag{6.52}$$

with $r = r_0$. Here gravitational force and centrifugal force just compensate each other.

$$F_{\mathrm{cf}} = M_{\mathrm{E}}\Omega^2 \cdot 0.75R \cdot \hat{r}_0 = -F_{\mathrm{G}}(r_0) \,.$$

The total force in M is zero (Fig. 6.53). This is no longer true for other points P because the distances to the moon are different and therefore the gravitational force differs while for the non-rotting earth the centrifugal force is the same for all points P. For example the gravitational force in the points A and B in Fig. 6.54 is

$$\begin{aligned} \boldsymbol{F}_{\mathrm{G}}(r_{\mathrm{A}}) &= -G\frac{m \cdot M_{\mathrm{Mo}}}{(r_0 + R)^2}\hat{\boldsymbol{r}}_0 \,, \\ \boldsymbol{F}_{\mathrm{G}}(r_{\mathrm{B}}) &= -G\frac{m \cdot M_{\mathrm{Mo}}}{(r_0 - R)^2}\hat{\boldsymbol{r}}_0 \,. \end{aligned} \tag{6.53}$$

Compared with the gravitational force $F_{\mathrm{G}}(r_0)$ in M the force differences are $\Delta F(r_{\mathrm{A}}) = F_{\mathrm{G}}(r_{\mathrm{A}}) - F_{\mathrm{G}}(r_0)$ and $\Delta F(r_{\mathrm{B}}) = F_{\mathrm{G}}(r_{\mathrm{B}}) - F_{\mathrm{G}}(r_0)$ which point in the direction of the connecting line earth–moon. The magnitude of these differences can be obtained from (6.52) and (6.53). Because $R \ll r_0$, we can approximate $(1 + R/r_0)^{-2} \approx 1 - 2R/r_0$ and we get:

$$\begin{aligned} \Delta\boldsymbol{F}(r_{\mathrm{A}}) &= -G \cdot \frac{m \cdot M_{\mathrm{Mo}}}{r_0^2} \cdot \left(\frac{1}{(1 + R/r_0)^2} - 1\right)\hat{\boldsymbol{r}}_0 \\ &\approx G \cdot \frac{2m \cdot M_{\mathrm{Mo}}}{r_0^3} R \cdot \hat{\boldsymbol{r}}_0 \\ &= -2\boldsymbol{F}_{\mathrm{G}}(r_0) \cdot \frac{R}{r_0} \cdot \hat{\boldsymbol{r}}_0 \,, \\ \Delta\boldsymbol{F}(r_{\mathrm{B}}) &= +2\boldsymbol{F}_{\mathrm{G}}(r_0) \cdot \frac{R}{r_0} \cdot \hat{\boldsymbol{r}}_0 \,, \end{aligned} \tag{6.54}$$

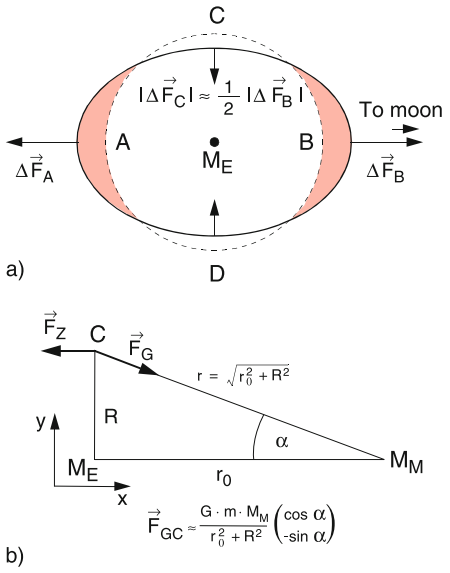

Figure 6.54 Deformation of the earth by the tides (exagerated). The *arrows* give magnitude and direction of the tidal forces

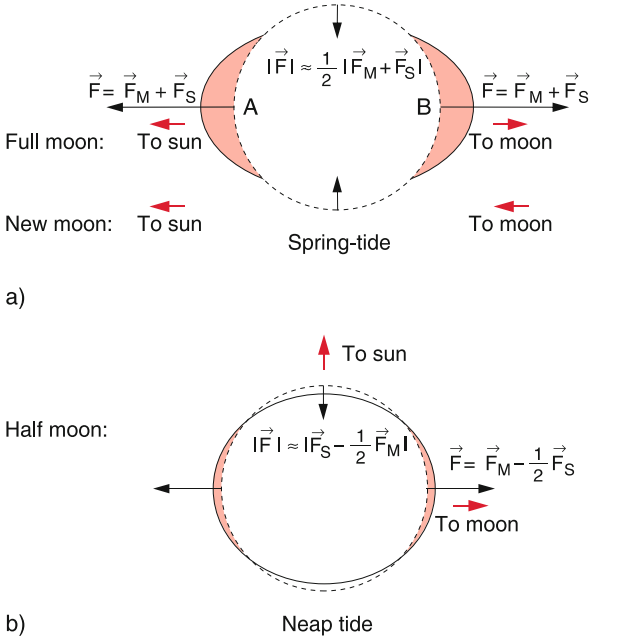

Figure 6.55 Spring tide and neap tide caused by addition or subtraction of the gravitational forces by moon and sun

The difference $\Delta F(r_B)$ is directed from M to the center of the moon, while $\Delta\boldsymbol{F}(r_A)$ has the opposite direction. Both differences result in a convex curved deformation of the earth surface, as shown exaggerated in Fig. 6.54. For a mass in the points C or D the gravitational force caused by the moon

$$\begin{aligned} \boldsymbol{F}_G(r_C) &= -G\frac{m \cdot M_{Mo}}{r_0^2 + R^2}\hat{\boldsymbol{r}} = \{F_x, F_y\} \\ &= F_G(r_0)\frac{r_0^2}{r_0^2 + R^2}\begin{pmatrix} \cos\alpha \\ -\sin\alpha \end{pmatrix} \end{aligned} \tag{6.55}$$

points to the center of the moon (Fig. 6.54b), while the centrifugal force is directed as for all points of the earth in the direction of r_0 and is anti-collinear to F_G, while the magnitude of both forces are equal, i.e. $\boldsymbol{F}_G(r_0) = -\boldsymbol{F}_{cf}$. (Note, that we regard a non-rotating earth and $\boldsymbol{F}_{cf}$ is only due to the revolution of earth and moon around the common center of mass S). With $\cos\alpha = r_0/\sqrt{(r_0^2 + R^2)}$ and $\sin\alpha = -R/\sqrt{(r_0^2 + R^2)}$ the resulting residual force is

$$\begin{aligned} \Delta\boldsymbol{F}(r_C) &= \boldsymbol{F}_{cf} + \boldsymbol{F}_G = F_G(r_0)\begin{pmatrix} \dfrac{r_0^3}{(r_0^2 + R^2)^{3/2}} - 1 \\ -\dfrac{r_0^2 R}{(r_0^2 + R^2)^{3/2}} \end{pmatrix} \\ &\approx F_G(r_0)\frac{R}{r_0}\begin{pmatrix} \frac{3}{2}(R/r_0) \\ -1 \end{pmatrix}, \end{aligned} \tag{6.56}$$

because $R \ll r_0 \Delta F(r_C)$ points nearly into the $-y$-directions to the center of the earth. it therefore decreases the curvature of the earth surface (Fig. 6.57b) which causes low tide. Its amount

$$\begin{aligned} \Delta F(r_C) &= |\boldsymbol{F}_G(r_C) - \boldsymbol{F}_G(r_0)| \approx G\frac{m \cdot M_{Mo}}{r_0^3}R \\ &= F_G(r_0) \cdot \frac{R}{r_0} = \frac{1}{2}\Delta F(r_A) \end{aligned} \tag{6.57}$$

is smaller by the factor $1/2$ than in the points A and B. For all other points of the earth surface the resulting forces ΔF have a radial as well as a tangential component. The tangential component causes an acceleration of the ocean water towards the points A or B. The borderline between the different tangential directions lies in Fig. 6.54a left of the line CD. where the x-component of F_G is

$$F_{Gr} = +\tfrac{3}{2}F_G(r_0)(R/r_0)\ . \tag{6.58}$$

From (6.54) and (6.56) one can infer, that the maximum tide force depends on the ratio M_{Mo}/r^3. If the numerical values for r and M_{Mo} are inserted one obtains $M_{Mo}/r^3 = 1.34 \cdot 10^{-3}\,\mathrm{kg/m^3}$ and a tide acceleration of $a_1 = \Delta F/m = 1.1 \cdot 10^{-6}\,\mathrm{m/s^2}$. This leads to a deformation of the solid earth crust of up to 0.5 m. Since $M_{sun}/r_{sun}^3 = 6.6 \cdot 10^{-4}\,\mathrm{kg/m^3}$ the effect of the sun on the tides is only about half of that of the moon and one obtains for the contribution to the tide-acceleration $a_2 = 5.6 \cdot 10^{-7}\,\mathrm{m/s^2}$. If sun and moon stand both on a line through the center of the earth (this is the case for full moon and for new moon) the actions of moon and sun add (spring-tide). If sun and moon are in quadrature (the connecting lines sun–earth and moon–earth intersect in the earth center under 90° (Fig. 6.55)) the effects subtract (neap tide).

Up to now, we have neglected the daily rotation of the earth. It brings about two effects:

- An additional centrifugal force, which causes the deformation of the earth into a oblate symmetric top (see Sect. 6.6.1) The deformation, which amounts to about 21 km at the equator, is very much larger than that caused by the moon but it is equal for all points on the same latitude and is not time dependent in contrast to the tides caused by the moon.

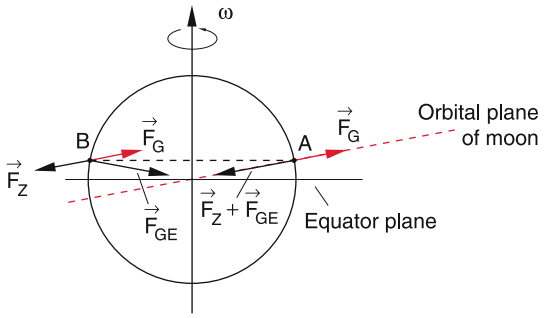

Figure 6.56 Influence of the inclination of the orbital plane of the moon on the periodical variation of the tidal elevation

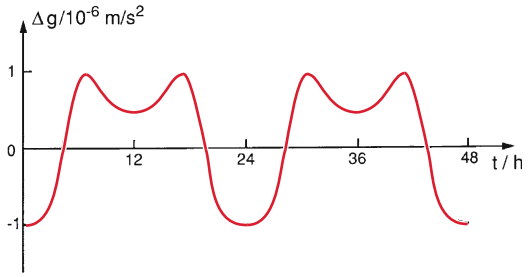

Figure 6.57 Time dependent course of the tidal elevation at a fixed point on the earth surface, measured as the corresponding variation Δg of the earth acceleration g

- When the revolution of the moon around the earth is ignored, the two tide maxima at the points A and B in Fig. 6.54 and the low tides in the point C and D would travel around the earth in 24 hours. At a fixed point one would experience every 12 hours a high tide and a low tide. The deformation of the solid crust is about 0.5 m, that of the ocean away from the coast about 1 m. Tide amplitudes up to 15 m are observed at the coast and in particular in narrow bays. They are generated by nonlinear effects during the propagation of tidal waves.

For a more accurate description of the tides the revolution of the moon has to be taken into account. It demands the following corrections of our simple model:

- The moon moves around the earth–moon-center of mass S in 27.5 days with the same direction as the rotation of the earth. Therefore, the round-trip time of the tides is 24.87 h instead of 24 h.
- The plane of the moon's revolution is inclined against the equator plane (Fig. 6.56). An observer in the point A experiences a higher tide amplitude than an observer in B 12.4 h later. This can be seen as follows: The centrifugal force (6.51) caused by the revolution of the earth–moon system around S is in A parallel to the gravitational force F_{GE} caused by the mass of the earth. The resulting force $F = F_{GE} + F_{GM} + F_{cf}$ is perpendicular to the earth surface. The total force has to include the centrifugal force F_{cE} caused by the rotation of the earth, which is perpendicular to the rotation axis of the earth. In the point B the centrifugal force F_{cf} has the same direction than in A, but the gravitational force F_{GE} has a nearly opposite direction and therefore the vector sum of the two forces is in B smaller than in A. The force F_{cE} has for both points the same direction because they are located on the same circle of latitude (Fig. 6.56). The tide amplitudes show an amplitude modulation with a period of about 12.4 h. The modulation index depends on the geographical latitude.
- The motion of the moon changes the relative positions of the interacting sun, moon and earth. Therefore, the vector sum of the tide forces show also a periodic modulation.

These considerations illustrate that the total tide amplitude is determined by the superposition of many effects and is therefore a complicated function of time (Fig. 6.57). It can be measured with various techniques. One of them uses the time variation of the gravitational acceleration g which depends on the geographic location and is affected by the tides. Another very sensitive interferometric technique measure the local deformation of the earth crust (see Sect. 6.6.4).

6.6.3 Consequences of the Tides

With the tides of the oceans as well as with the periodic deformations of the earth crust, friction occurs which causes a partial transfer of kinetic energy into heat. This lost kinetic energy slows down the rotation of the earth and causes an increase of the rotation period by 90 ns per day. Within 10^6 years this prolongs the duration of the day by 0.5 min (see Probl. 1.4).

The gravitational force between earth and moon causes of course also deformations on the moon. Accurate measurements have proved that the shape of the moon is an ellipsoid with the major axis pointing towards the earth. The general opinion is that in former times the moon also rotated around its axis. This rotation was, however, in the course of many million years slowed down by friction until the moon no longer rotates and shows always the same side to the earth.

The tidal friction of earth and moon has the following interesting effect: The total angular momentum of the earth–moon system is constant in time because the system moves in the central force field of the sun (the additional non-central forces due to interactions with the other planets are negligible). Since the rotation of the earth around its axis slows down and its angular momentum $I \cdot \omega$ decreases, the orbital angular momentum of the earth–moon system

$$|\boldsymbol{L}_{EM}| = r \cdot \mu \cdot v_{rel} \cdot = I_{EM} \cdot \Omega$$

(r = distance earth–moon, v_{rel} = relative velocity of the moon against the earth, I_{EM} = inertial moment of the earth–moon system and Ω = angular velocity of the rotating earth–moon system) has to increase. The moon is accelerated by the tidal wave running around the earth. This can be seen as follows (Fig. 6.58): The earth rotating with the angular velocity $\omega \gg \Omega$ accelerates the tidal waves due to the friction forces: This acceleration brings the tidal maximum slightly ahead of the connecting line between the centers of earth and moon. Due to the slightly increased gravitational force, the moon is accelerated while the earth rotation decreases. The larger kinetic energy

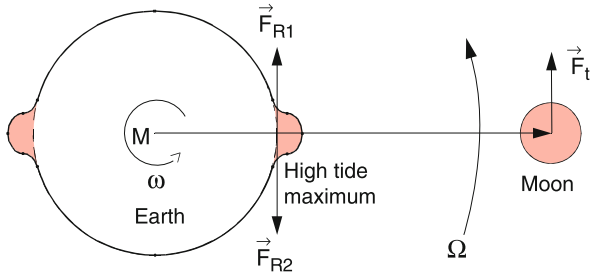

Figure 6.58 Deceleration of the earth rotation and acceleration of the orbital velocity of the moon by the tidal friction

of the moon increases its total energy ($E_{kin} + E_{pot}$) and therefore also its distance to the earth. In former times the moon was closer to the earth. The nowadays generally accepted theory [6.7a, 6.7b] assumes that the moon was part of the earth but has been catapulted out of the earth by the impact of a heavy asteroid some billion years ago (see Vol. 4).

6.6.4 Measurements of the Earth Deformation

The deformation of the earth by tidal effects can be measured with different techniques. We will shortly discuss three of them:

6.6.4.1 Changes of the Gravitational Force

According to (6.54) the additional gravitational force caused by the moon in the points A and B in Fig. 6.54 is

$$\Delta F_G \approx \frac{2mM_{Mo}}{r_{Mo}^3} R \,. \tag{6.59}$$

In the gravity meter shown in Fig. 6.59 a mass m is suspended by a spring in such a way, that a small change $\Delta F_G = m \cdot \Delta g$ due to the corresponding change of g causes a large vertical deflection of the arrow on the scale. This is achieved by a sloped mounting of the spring with length L and a restoring force $F_r = -D \cdot \Delta L$. With the slope angle α, the vertical deflection Δz causes a length increase of the spring $\Delta L = \Delta z \cdot \sin\alpha$ (Fig. 6.59b) and a change of the restoring force $\Delta F_r = m \cdot \Delta g \cdot \sin\alpha$.

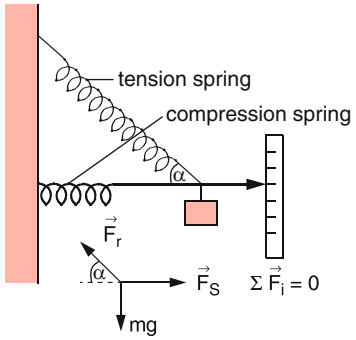

Figure 6.59 Measurement of the gravitational force with a special spring balance

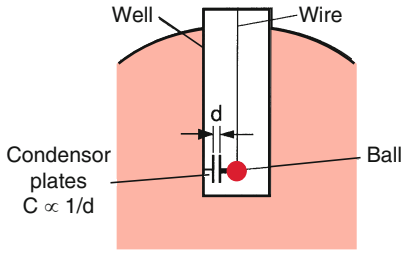

Figure 6.60 Measurement of the deviation of g from the vertical direction

The device measures the periodic changes of F_G with a period of 24.87 h from which the tidal amplitudes can be inferred (Fig. 6.57). Because of the different contributing effects, $\Delta g(t)$ follows a complicated curve.

The experimental arrangement of Fig. 6.60 allows to measure the deviation from the vertical direction of the earth acceleration g. Without external perturbation, g would point nearly to the earth center (only for a spherical mass distribution it would point exactly to the center). The additional gravitational force exerted by the moon causes a slight deviation from this direction. The maximum angular deviation, which depends on the latitude, amounts only to about $2.1 \cdot 10^{-6}$ rad$(= 0.4'')$, the measurement must be sufficiently accurate. This required accuracy can be reached with a pendulum [6.9]. A metal ball suspended on a long wire in a well is connected with one plate of a charged capacitor, while the other plate is fixed on the wall of the well. Any deviation of the pendulum from the vertical direction changes the distance between the two plates and therefore the voltage of the capacitor (see Vol. 2, Sect. 5).

6.6.4.2 Measurements of the Earth Deformation

Here the change ΔL of the length L between two points A_1 and A_2 connected with the earth ground is measured. Figure 6.61 illustrates the method. A very sensitive Laser interferometer is located in a gold mine deep in the ground in order to eliminate acoustic noise from the surroundings. The two mirrors of the laser resonator are mounted on the ground base at the points A_1 and A_2 separated by the distance L. The optical frequency of the laser $\nu_L = m \cdot c/(2L)$ is determined by the length L of the resonator and the large integer $m \gg 1$. If the length L changes due to the deformation of the earth crust, the laser frequency changes accordingly. This frequency change can be measured very accurately, when the laser beam is superimposed on a detector with the output beam of a reference laser with stabilized frequency ν_r. The difference frequency $\nu_L - \nu_r$ in the radio-frequency range can be counted by a digital frequency counter. Existing devices have resonator lengths of 100 m up to several km. They can measure deformations of the earth crust of less than 10^{-9} m (see Vol. 2, Sect. 10.4). This sensitivity is sufficient to measure the deformation of the ground base in the Rocky Mountains caused by the tidal waves of the Pacific Ocean [6.10].

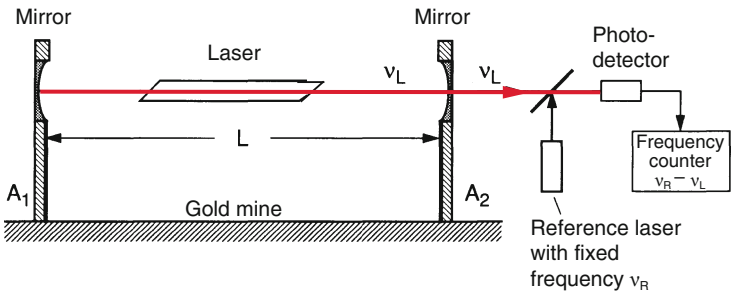

Figure 6.61 Laser interferometer for the measurement of the deformation of the earth crust

Summary

- Elastic bodies show restoring forces for any deformation of their shape. For sufficiently small deformations, these forces are proportional to the elongation from the equilibrium position.
- For a relative length increase $\varepsilon = \Delta L/L$ of a body with length L, constant cross section and elastic modulus E one needs a tensile stress $\sigma = E \cdot \varepsilon$ (Hooke's law).
- A length change ΔL of a rod with length L and quadratic cross section $A = d^2$ caused by the tensile stress σ is accompanied by a change ΔA of its cross section. The relative change of the volume V

$$\frac{\Delta V}{V} = \frac{\sigma}{E}(1 - 2\mu)$$

  is determined by the elastic modulus E and the transvers contraction ratio $\mu = -(\Delta d/d)/(\Delta L/L)$.
- Exposed to isotropic pressure p the relative volume change $\Delta V/V = -\kappa \cdot p$ of a body is determined by the compressibility $\kappa = (3/E) \cdot (1 - 2\mu)$.
- A force F acting tangentially on a wall of a body causes a shear of the body. For a cuboid with the side area d^2 the shear angle α is related to the shear stress $\tau = F/d^2$ by $\tau = G \cdot \alpha$ where G is the modulus of shear.
- A rod with length L and cross section $d \cdot b$ is fixed at one end. The vertical force $\boldsymbol{F}$ acting on the other end causes a bending

$$s = (4L^3 \cdot F)/(E \cdot d^3 \cdot b) \ ,$$

  which is proportional to the third power of the length L and the vertical width d.
- Beyond the linear range of Hooke's law plastic deformations occur. If a periodical tensile stress σ acts on a rod with length L, a closed hysteresis curve $\sigma(\varepsilon)$ is traversed. The area enclosed by this curve represents the energy that is transformed into heat for every cycle.
- Inside a liquid the same pressure is present for all volume elements with the same distance Δh from the surface. The hydrostatic pressure $p(z) = p_0 + \varrho \cdot g \cdot (h - z)$ at this height increases linearly with the height $(h - z)$ of the liquid with density ϱ above the layer at z. At the upper surface $z = H$ of a liquid with total height H the pressure is p_0 (for example the barometric pressure of the air above the surface).
- Each solid body with mass m and density ϱ_s experience in a liquid a buoyant force $\boldsymbol{F}_B$ which is equal but opposite to the weight $\boldsymbol{F}_G$ of the liquid volume displaced by the solid body. If $|\boldsymbol{F}|_B > m \cdot g$ the body floats at the liquid surface, for $|\boldsymbol{F}_B| = m \cdot g$ the body can float at any height in the liquid.
- Because of the attractive forces between the molecules of a liquid, energy is required to bring molecules from the interior to the surface. The energy, necessary to increase the surface by $1\,m^2$, is the specific surface energy. It is equal to the specific surface tension.
- The shape of the surface of a liquid in a container depends on the different surface tensions for the boundaries between container wall and liquid, liquid and air, container wall and air and on the gravity force. It always takes that form, for which the energy is minimum.
- Because of the surface tension a liquid can rise in a capillary (wetting liquid) or descend (non-wetting liquid).
- When two bodies come into touch, friction forces appear, which are different for a relative velocity zero (static friction) or for a relative motion (sliding friction). The smallest friction is found, when a circular body rolls on a plane base. The quantitative description uses friction coefficients μ, which depend on the materials of the two bodies. Generally it is $|\mu_s| > |\mu_{sl}| > |\mu_R|$, where μ_s is the coefficient for static friction, μ_{sl} for sliding friction and μ_R for rolling friction. A liquid film between the two solid bodies reduces the friction considerably.
- The earth is a deformable ellipsoid which is permanently deformed by its rotation and periodically by the gravitational forces exerted by moon and sun, which cause tidal effects. The periodic deformations are partly non-elastic and the friction transfers part of the rotational energy into heat. This causes a slowdown of the earth rotation and a prolongation of the day. Conservation of the total angular momentum leads to an increase of the distance earth–moon.

Problems

6.1 What is the change ΔL of a steel rope with $L = 9\,\text{km}$,
a) which hangs in a vertical well?
b) What is the maximum length of the rope before its rupture?
c) How large is ΔL when the rope is lowered from a ship into the ocean? ($E = 2 \cdot 10^{11}\,\text{N/m}^2$; $\varrho_{\text{steel}} = 7.7 \cdot 10^3\,\text{kg/m}^3$, $\varrho_{\text{ocean}} = 1.03 \cdot 10^3\,\text{kg/m}^3$)

6.2 A steel beam with $L = 10\,\text{m}$ is clamped at one end. A force $F = 10^3\,\text{N}$ acts on the other end in vertical z-direction. How large is the bending of this end
a) for a rectangular cross section $d \cdot b$ with $d = \Delta z = 0.1\,\text{m}$; $b = \Delta y = d/2$?
b) for a double T-profile (Fig. 6.15d) with $b_1 = d_1 = 0.1\,\text{m}$, $b_2 = d_2 = 0.05\,\text{m}$?

6.3 The deep ocean aquanaut Picard reached in his spherical steel submarine a depth of 10.000 m in the Philippine trench. How large are pressure and total force exerted on the sphere? What is the volume change $\Delta V/V$ caused by the pressure
a) for a hollow sphere with wall thickness of 0.2 m?
b) for a full sphere?

6.4 A turbine drives a generator connected to a steel shaft with length L and diameter D. By which angle α are the two ends of the shaft twisted if the power $P = 300\,\text{kW}$ is transferred at a frequency $\omega = 2\pi \cdot 25\,\text{s}^{-1}$
a) for a steel shaft as full cylinder with $D = 0.1\,\text{m}$; $L = 20\,\text{m}$?
b) for a hollow cylinder with $D_1 = 5\,\text{cm}$ and $D_2 = 10\,\text{cm}$?

6.5 What is the density of water with a compressibility $\kappa = 4.8 \cdot 10^{-10}\,\text{m}^2/\text{N}$ at a depth of 10.000 m?

6.6 A hollow steel cube ($\varrho = 7.8 \cdot 10^3\,\text{kg/m}^3$) with edge length $a = 1\,\text{m}$ and a wall thickness of $d = 0.02\,\text{m}$ and with an open upper side floats on water.
a) How deep does it immerse?
b) What is the location of center of mass and metacenter?
c) What is the maximum angle of its symmetry axis against the vertical direction before it becomes unstable?

6.7 Which energy has to be spent in order to lift a full cube of steel from the bottom of a swimming pool with the water depth of 4 m to a position where the lower side of the cube is at the surface of the water?

6.8 Which force was necessary to separate the two hemispheres in the demonstration experiment by Guericke in Magdeburg with a diameter of 0.6 m, when the pressure difference between inside and outside was $\Delta p = 90\,\text{kPa}$? Guericke had used 16 horses. What should have been done in order to separate the hemi-spheres already with 8 horses?

6.9 In order to verify that a gold bar is really made of gold ($\varrho_{\text{gold}} = 19.3\,\text{kg/dm}^3$) a goldsmith measures its weight in air and when totally immersed in water. Which ratio of the two values is obtained
a) for a 100% gold bar?
b) for a 20% admixture of copper ($\varrho = 8.9\,\text{kg/dm}^3$)?
c) What is the minimum required accuracy of the measurements for unambiguously distinguishing between the two cases? What is the accuracy if an admixture of 1% of copper should be detected?

6.10 A round cylinder of wood ($L = 1\,\text{m}$, $d = 0.2\,\text{m}$, $\varrho = 525\,\text{kg/m}^3$) is floating in water. How deep does it immerse
a) in a horizontal position?
b) if a steel ball with $m = 1\,\text{kg}$ is attached to one end in order to bring it into a vertical floating position?

References

6.1. W.D. Callister, D.G. Rethwisch, *Material Science and Engineering. An Introduction.* (Wiley, 2013)
6.2. *Deformation,* ed. by M. Hazewinkel *Encyclopedia of Mathematics.* (Springer, 2001)
6.3. S. Lipschitz, *Schaum's Outline of mathematical Handbook of Formulas.* (McGraw Hill, 2012)
6.4. M. Abramowitz, I. Stergun, *Handbook of Mathematical Functions.* (Martino Fine Books)
6.5. R.H. Rapp, F. Sanso (ed.), *Determination of the Geoid.* (Springer, Berlin, Heidelberg, 1991)
6.6a. V.M. Lyathker, *Tidal Power. Harnessing Energy from Water Currents.* (Wiley Scrivener, 2014)
6.6b. L. Peppas, *Ocean, Tidal and Wave energy.* (Crabtree Publ. Comp., 2008)
6.6c. https://en.wikipedia.org/wiki/List_of_tidal_power_stations
6.6d. https://en.wikipedia.org/wiki/Tidal_power
6.7a. http://novan.com/earth.htm
6.7b. P. Brosche, H. Schuh, Surveys in Geophysics **19**, 417 (1998)

6.8a. D. Flannagan, *The Dynamic Earth.* (Freeman, 1983)
6.8b. G.M.R. Fowler, *The Solid Earth. An Introduction to Global Geophysics.* (Cambridge Univ. Press, 2004)
6.9. D. Wolf, M. Santoyo, J. Fernadez (ed.), *Deformation and Gravity Change.* (Birkhäuser, 2013)
6.10. J. Levine, J.L. Hall, J. Geophys. Res. **77**, 2595 (1972)
6.11. A.E. Musset, M.A. Khan, *Looking into the Earth: An Introduction to Geological Geophysics.* (Cambridge Univ. Press, 2000)
6.12. M. Goldsmith, M.A. Garlick, *Earth: The Life on our Planet.* (Kingfisher, 2011)